



# Baseline circulating unswitched memory B cells and B-cell related soluble factors are associated with overall survival in patients with clear cell renal cell carcinoma treated with nivolumab within the NIVOREN GETUG-AFU 26 study

Lucia Carril-Ajuria <sup>1,2</sup>, Aude Desnoyer,<sup>2,3</sup> Maxime Meylan,<sup>4</sup> Cécile Dalban,<sup>5</sup> Marie Naigeon,<sup>3,6,7</sup> Lydie Cassard,<sup>2</sup> Yann Vano,<sup>4,8</sup> Nathalie Rioux-Leclercq,<sup>9</sup> Salem Chouaib,<sup>10</sup> Benoit Beuselinck,<sup>11</sup> Sylvie Chabaud,<sup>5</sup> Janice Barros-Monteiro,<sup>12</sup> Antoine Bougoüin,<sup>4</sup> Guillaume Lacroix,<sup>4</sup> Irelka Colina-Moreno,<sup>4</sup> Florence Tantot,<sup>13</sup> Lisa Boselli,<sup>2</sup> Caroline De Oliveira,<sup>2</sup> Wolf Herve Fridman <sup>4</sup>, Bernard Escudier,<sup>1</sup> Catherine Sautes-Fridman <sup>4</sup>, Laurence Albiges,<sup>1,7</sup> Nathalie Chaput-Gras<sup>2,3</sup>

**To cite:** Carril-Ajuria L, Desnoyer A, Meylan M, *et al.* Baseline circulating unswitched memory B cells and B-cell related soluble factors are associated with overall survival in patients with clear cell renal cell carcinoma treated with nivolumab within the NIVOREN GETUG-AFU 26 study. *Journal for ImmunoTherapy of Cancer* 2022;**10**:e004885. doi:10.1136/jitc-2022-004885

► Additional supplemental material is published online only. To view, please visit the journal online (<http://dx.doi.org/10.1136/jitc-2022-004885>).

LC-A and AD contributed equally. LA and NC-G contributed equally.

Accepted 23 April 2022



© Author(s) (or their employer(s)) 2022. Re-use permitted under CC BY-NC. No commercial re-use. See rights and permissions. Published by BMJ.

For numbered affiliations see end of article.

## Correspondence to

Dr Nathalie Chaput-Gras; CHAPUT-GRAS.Nathalie@gustaveroussy.fr

## ABSTRACT

**Background** The phase II NIVOREN GETUG-AFU 26 study reported safety and efficacy of nivolumab in patients with metastatic clear cell renal cell carcinoma (m-ccRCC) in a 'real-world setting'. We conducted a translational-research program to determine whether specific circulating immune-cell populations and/or soluble factors at baseline were predictive of clinical outcomes in patients with m-ccRCC treated with nivolumab within the NIVOREN study.

**Methods** Absolute numbers of 106 circulating immune-cell populations were prospectively analyzed in patients treated at a single institution within the NIVOREN trial with available fresh-whole-blood, using dry formulation panels for multicolor flow cytometry. In addition, a panel of 14 predefined soluble factors was quantified for each baseline plasma sample using the Meso-Scale-Discovery immunoassay. The remaining patients with available plasma sample were used as a validation cohort for the soluble factor quantification analysis. Tumor immune microenvironment characterization of all patients included in the translational program of the study was available. The association of blood and tissue-based biomarkers, with overall survival (OS), progression-free survival (PFS) and response was analyzed.

**Results** Among the 44 patients, baseline unswitched memory B cells (NSwM B cells) were enriched in responders ( $p=0.006$ ) and associated with improved OS (HR=0.08,  $p=0.002$ ) and PFS (HR=0.54,  $p=0.048$ ). Responders were enriched in circulating T follicular helper (Tfh) ( $p=0.027$ ) and tertiary lymphoid structures (TLS) ( $p=0.043$ ). Circulating NSwM B cells positively correlated with Tfh ( $r=0.70$ ,  $p<0.001$ ). Circulating NSwM B cells correlated positively with TLS and CD20 +B cells at the tumor center ( $r=0.59$ ,  $p=0.044$ , and  $r=0.52$ ,  $p=0.033$ )

and inversely correlated with BCA-1/CXCL13 and BAFF ( $r=-0.55$  and  $r=-0.42$ ,  $p<0.001$ ). Tfh cells also inversely correlated with BCA-1/CXCL13 ( $r=-0.61$ ,  $p<0.001$ ). IL-6, BCA-1/CXCL13 and BAFF significantly associated with worse OS in the discovery ( $n=40$ ) and validation cohorts ( $n=313$ ).

**Conclusion** We report the first fresh blood immune-monitoring of patients with m-ccRCC treated with nivolumab. Baseline blood concentration of NSwM B cells was associated to response, PFS and OS in patients with m-ccRCC treated with nivolumab. BCA-1/CXCL13 and BAFF, inversely correlated to NSwM B cells, were both associated with worse OS in discovery and validation cohorts. Our data confirms a role for B cell subsets in the response to immune checkpoint blockade therapy in patients with m-ccRCC. Further studies are needed to confirm these findings.

## BACKGROUND

Immunotherapy, particularly immune checkpoint blockade (ICB) therapy, has revolutionized the landscape of systemic therapy across different solid tumors by boosting the effector T cell responses.<sup>1</sup> Immune checkpoint inhibitors have the potential to provide sustained responses and long-term survival in different solid tumors, including metastatic clear cell renal cell carcinoma (m-ccRCC).<sup>2</sup> However, only a subset of patients will benefit from these treatments.<sup>3-6</sup> The understanding of the underlying mechanisms of the antitumor immune response and the identification of

reliable biomarkers of response to ICB has therefore become a major goal of immunotherapy research.

To date, there is still no validated biomarker of response to ICB for m-ccRCC.<sup>2</sup> Until recently, the search of biomarkers had mainly focused on T cells and tumor cells, and mostly at tissue level.<sup>7-9</sup> Despite its success in other solid tumors, and its ability to enrich for response to ICB doublet in m-ccRCC, the programmed death ligand-1 (PD-L1) expression is not routinely used as a predictive factor in m-ccRCC.<sup>2, 10</sup> Likewise, the tumor mutational burden has been postulated as a promising biomarker in non-small cell lung cancer (NSCLC) and other solid tumors, however it was not confirmed in m-ccRCC.<sup>8, 11</sup> Immune signatures have actively been developed across trials; however, they are still not ready for incorporation into routine clinical practice.<sup>7, 9, 12</sup>

As main protagonists and targets of ICB therapy, infiltrating-cytotoxic T cells have been largely investigated, however the results in m-ccRCC are controversial.<sup>7, 8</sup> Growing evidence supports the role of other immune players in the antitumor response, such as myeloid-derived suppressor cells or B lymphocytes.<sup>13, 14</sup> Infiltrating B cells have been detected in different solid tumors, including m-ccRCC.<sup>13, 15</sup> The role of these cells is still under debate.<sup>16, 17</sup> Some studies highlight the immune-inhibitory functions of the tumor-associated B cells which may behave as regulatory B cells inhibiting the inflammatory antitumor response and even inducing tumor heterogeneity and therapy resistance.<sup>18-20</sup> Other studies suggest that B cell subpopulations promote and sustain tumor inflammation and are implicated in antigen presentation, T cell activation, and cytokine production.<sup>16, 17</sup> Additionally, there is increasing evidence that tumor infiltrating B cells, especially those present with T cells in organized lymphoid aggregates called tertiary lymphoid structures (TLS), correlate with better prognosis.<sup>13, 21</sup> Furthermore, five recently reported studies have shown an association of B cells and TLS with clinical outcomes in patients with cancer treated with ICB.<sup>17, 22-25</sup> Specifically, in the study conducted by Helmink and colleagues, tumors from responder patients were enriched in memory B cells and presented increased plasma cells compared with tumors from non-responders.<sup>17</sup> These data suggest that B cell subpopulations within the TLS may modulate the T cell antitumor response and represent a potential marker of response to ICB.

In contrast to tissue-based markers, the identification of blood-based biomarkers, has emerged as a promising approach given their availability and the potential to be a better reflection of the host and tumor immune status at a specific time point. Thus, among blood-based biomarkers, circulating immune cells and soluble factors have also been investigated.<sup>14, 26-29</sup> Data on the role of circulating B cells and antitumor response are scarce. Total circulating B cell pool mainly consists of naive B cells (CD19+, CD27-, IgD+, IgM+), double negative B cells (DN B cells, CD19+, CD27-, IgD-/IgM-) and memory B cells including unswitched (NSwM, CD19+,

CD27+, IgD+, IgM+) and switched memory B cells (SwM B cells, CD19+, CD27+, IgD-, IgM-). A retrospective study including different cancer types treated with ICB, reported that levels of pretreatment circulating B cells correlated negatively with response to ICB.<sup>26</sup> However, the correlation of the different circulating B cell subsets with the response to ICB was not evaluated in m-ccRCC. Very recently, Xia *et al* identified IgM+ memory B cells as predictors of response to anti-programmed cell death protein-1 (PD-1) treatment in advanced NSCLC.<sup>30</sup>

The aim of our study was to determine whether specific immune cell populations and/or soluble factors at baseline were predictive of clinical outcomes to ICB in m-ccRCC. Therefore, we characterized immune-cell populations in fresh-whole-blood and performed circulating soluble factors quantification at baseline in patients with m-ccRCC treated with nivolumab within the phase II NIVOREN GETUG-AFU 26. Furthermore, tumor immune microenvironment (TIME) characterization was correlated with blood-based biomarkers.

## PATIENTS AND METHODS

### Patient cohorts and sample collection

This study was conducted as part of the translational program of the multicenter, prospective, phase II NIVOREN GETUG-AFU 26 trial (EudraCT n°: 2015-004117-24/03013335) (online supplemental figure S1). Seven hundred and twenty-nine patients with m-ccRCC previously treated with at least one anti-angiogenic were included in this trial. Patients received nivolumab monotherapy 3 mg/kg every 2 weeks until death, disease progression, unacceptable toxicity, or withdrawal of the informed consent. Response was assessed every 12 weeks by RECIST V.1.1.

Six hundred and seventeen patients out of the 729 patients included in this trial took part in the translational program. The study design included the collection of patient's clinical data, blood samples at baseline, at 1 month and at end of treatment (EOT) (including fresh blood samples for the patients treated at the Institute Gustave Roussy (IGR)), and tumor tissue samples, after signature of informed consent. This study was conducted in accordance with ethical principles for medical research involving human subjects reported in the Declaration of Helsinki.

For the fresh blood immune-phenotyping and soluble factors quantification analysis, all consecutive 44 patients of the trial treated at a single institution (IGR) and enrolled in the translational study were defined as the discovery cohort. For the immunohistochemistry (IHC) analysis, 324 patients with centrally confirmed clear cell renal cell carcinoma tumor tissue (>50% tumor cells) were included (PRTK cohort). Seventeen patients were included in both the fresh blood immune-phenotyping and IHC analysis. The results of the soluble factor quantification analysis were confirmed in an independent validation cohort

including 313 patients where plasma samples were available.

### Multicolor flow cytometry

The procedures to perform blood immune phenotyping on fresh-whole-blood samples and flow cytometry antibodies and fluorochromes used are described in the online supplemental methods and table S1, respectively. Unsupervised analysis of flow cytometry data were performed using t-distributed stochastic neighbor embedding (t-SNE) algorithm with the online R software (V.3.5.0, cytofkit2 package). After setting the compensation matrix, CD19<sup>+</sup>CD3<sup>+</sup> cells events were extracted and software transformation was applied, t-SNE analysis was achieved on 2000 CD19<sup>+</sup> for each sample, using 'B-cell' panel markers. Flow cytometry gating strategy were performed as previously described.<sup>31</sup> Supervised analysis of flow cytometry data were performed using Kaluza Flow Cytometry Software (Beckman Coulter) and was done by a single operator, blinded to the clinical patients' information. Graphs for flow cytometry data were performed by GraphPad Prism V.8.0 (GraphPad Software) and by R software (V.4.1.1; package corrplot).

### Soluble factors quantification analysis

Peripheral blood samples were obtained from each patient prior to the first dose of nivolumab. Plasma samples of the patients included in the analysis were separated using centrifugation in cell preparation tubes, then frozen at  $-80^{\circ}\text{C}$  for subsequent analysis. A panel of 14 predefined different soluble factors involved in inflammation (vascular endothelial growth factor (VEGF), vascular cell adhesion molecule (VCAM-1), interleukin (IL)-6, IL-8, macrophage-derived chemokine (MDC), interferon (IFN)-gamma and tumor necrosis factor (TNF)-alpha), early T-cell development (IL-7), T-cell activation (4-1BB), immunosuppression (IL-10), hematopoiesis regulation (stromal cell-derived factor-1 (SDF-1)) and in B cell survival/differentiation (BAFF, BCA-1/CXCL13, APRIL) were quantified for each plasma sample using the Meso Scale Discovery (MSD) immunoassay according to the manufacturer recommendations. The procedures and the different kits used to perform the soluble factor quantification using the MSD immunoassay, as well as the lower limits of detection can be found in online supplemental methods and table S1.

### Immunohistochemistry and immune cells densities

All immunostainings were performed on  $3\ \mu\text{m}$  thick whole sections prepared from formalin-fixed paraffin-embedded blocks using Autostainer Dako. Antigen retrieval and deparaffinization was carried out on a PT-Link (Dako) using the EnVision FLEX Target Retrieval Solutions (Dako). The following primary antibodies were used: CD20 (Dako, Clone L26,  $0.6\ \mu\text{g}/$

mL), CD3 (Dako Rabbit polyclonal  $7.5\ \mu\text{g}/\text{mL}$ ) and CD8 (Dako Clone C8/144B,  $1.6\ \mu\text{g}/\text{mL}$ ). Chromogenic detection of TLS was performed using HighDef red IHC chromogen (AP) (Enzo, ADI-950-140-0030) for CD20, Permanent HRP Green (Zytomed Systems, ZUC070-100) for CD3 and using DAB (3,3 diaminobenzidine, Dako) linked secondary antibodies for CD8. The nuclei were counterstained with hematoxylin (Dako, S3301). After mounting with EcoMount (Biocare Medical, EM897L), the slides were scanned with a NanoZoomer (Hamamatsu). By using Halo 10 software (Indicalab), a first layer was created to define tumor area. Cell densities were quantified and a classifier to detect intratumoral TLS with surface area equal or above  $7000\ \mu\text{m}^2$  and containing at least 100 cells was created to count number and density of TLS/tumorous area. Results were validated blindly by two additional observers (GL, AB).

### Bioinformatics and statistical analysis

Descriptive statistics were used to summarize patient's characteristics. Statistical analysis of supervised flow cytometry cell population's analysis was performed after data adjustment by  $\log_2$ . Variables were summarized as proportions for categorical variables, the median and IQR, minimum and maximum for continuous variables. Objective response rate was defined as the percentage of patients achieving partial or complete response. The relationship between two categorical variables was estimated with the  $\chi^2$  test, or the Fisher's exact test for low frequencies. The relationship between two quantitative variables was estimated by Pearson correlation. Progression-free survival (PFS) was defined as the time between treatment initiation and first progression or death, and overall survival (OS) was defined as the time between treatment initiation and death or date of last follow-up. OS and PFS were estimated with the Kaplan-Meier method and were described in terms of median or specific time point estimation in each subgroup, along with the associated two-sided 95% CI for the estimates and were compared with the log-rank test. Median follow-up was estimated by reverse Kaplan-Meier method. Cox proportional hazards regression model was used to estimate HR and 95% CI. All p values were two-sided, and values less than 0.05 were considered statistically significant. Statistical analyses were performed using SAS V.9.4 and R Software (V.3.4.4).

## RESULTS

### Patient's characteristics and clinical outcomes

Fresh blood immune-phenotyping was prospectively conducted on 44 consecutive patients included in NIVOREN GETUG-AFU 26 trial at the IGR between January 2016 and July 2017. Quantitative analysis of tumor IHC was available for 18 patients of this discovery cohort. Patient's characteristics and clinical

**Table 1** Patient's baseline characteristics and clinical outcomes

	Discovery cohort N=44	Validation cohort N=313	Overall study population N=720
mAge (years)	61.5 (33.0–81.0)	64.0 (22.0–87.0)	64.0 (22.0–90.0)
Sex			
Men	29 (65.9)	251 (80.2)	556 (77.2)
Female	15 (34.1)	62 (19.8)	164 (22.8)
Score IMDC			
Favorable	20 (45.5)	50 (16.0)	131 (18.2)
Intermediate	17 (38.6)	178 (57.1)	404 (56.3)
Poor	7 (15.9)	84 (26.9)	183 (25.5)
ECOG PS			
<2	39 (88.6)	254 (85.2)	581 (84.9)
≥2	5 (11.4)	44 (14.8)	103 (15.1)
Fuhrman grade			
I	2 (4.7)	14 (5.0)	27 (4.1)
II	11 (25.6)	83 (29.5)	192 (29.5)
III	17 (39.5)	127 (45.2)	295 (45.3)
IV	13 (30.2)	57 (20.3)	136 (20.9)
Sarcomatoid component			
Yes	5 (11.4)	26 (9.0)	58 (8.5)
No	39 (88.6)	262 (91.0)	626 (91.5)
Nephrectomy	42 (95.5)	263 (84.0)	609 (84.6)
Brain metastases	9 (20.5)	42 (14.5)	83 (12.3)
Previous therapy lines			
1	28 (63.6)	179 (57.2)	359 (49.9)
2–3	11 (25.0)	112 (35.8)	295 (40.9)
>3	3 (6.8)	22 (7.0)	66 (9.1)
ORR	7 (17.9)	60 (19.2)	144 (21.0)
12 months PFS (% , 95% CI)	20.5 (10.1 to 33.0)	24.6 (20.0 to 29.5)	23.8 (20.7 to 27.0)
12 months OS (% , 95% CI)	84.0 (69.4 to 92.0)	69.0 (63.5 to 73.8)	69.4 (65.9 to 72.7)

IHC, immunohistochemistry; IMDC, International Metastatic RCC Database Consortium; mAge, median age; ORR, objective response rate; OS, overall survival; PFS, progression-free survival; ECOG PS, Eastern Cooperative Oncology Group performance status.

outcomes of the discovery cohort, validation cohort and the overall study population included in this trial are reported in [table 1](#).

In general, the baseline demographic and clinical characteristics of the validation cohort and the overall study population were similar ([table 1](#)). Compared with the overall study population, the discovery was enriched in favorable-risk patients, 45% compared with the validation and the overall study population cohorts (16% and 18%, respectively) ([table 1](#)). Brain metastases were more frequent in the discovery cohort, 20% compared with 12%–14% in the validation and overall study population cohorts. Objective response rate and PFS were similar among the three cohorts of patients. The discovery cohort presented a

superior 12 months OS rate than the validation cohort and overall study population ([table 1](#)).

#### Circulating B cells subpopulations and response to nivolumab in m-ccRCC

T-SNE algorithm, performed on the first consecutive six patients with OR (responders) and six patients with no-OR (non-responders) to nivolumab, showed that patients who responded had a higher density of CD19 +CD27+IgD+IgM +cells (assimilated to unswitched (or non-switched) memory B cells (NSwM B cells)), CD19 +CD27+IgD–IgM–cells (assimilated to switched memory B cells (SwM B cells)) and CD19 +CD27–IgD–IgM–cells (assimilated to double negative B cells (DN B cells)) ([figure 1](#)).

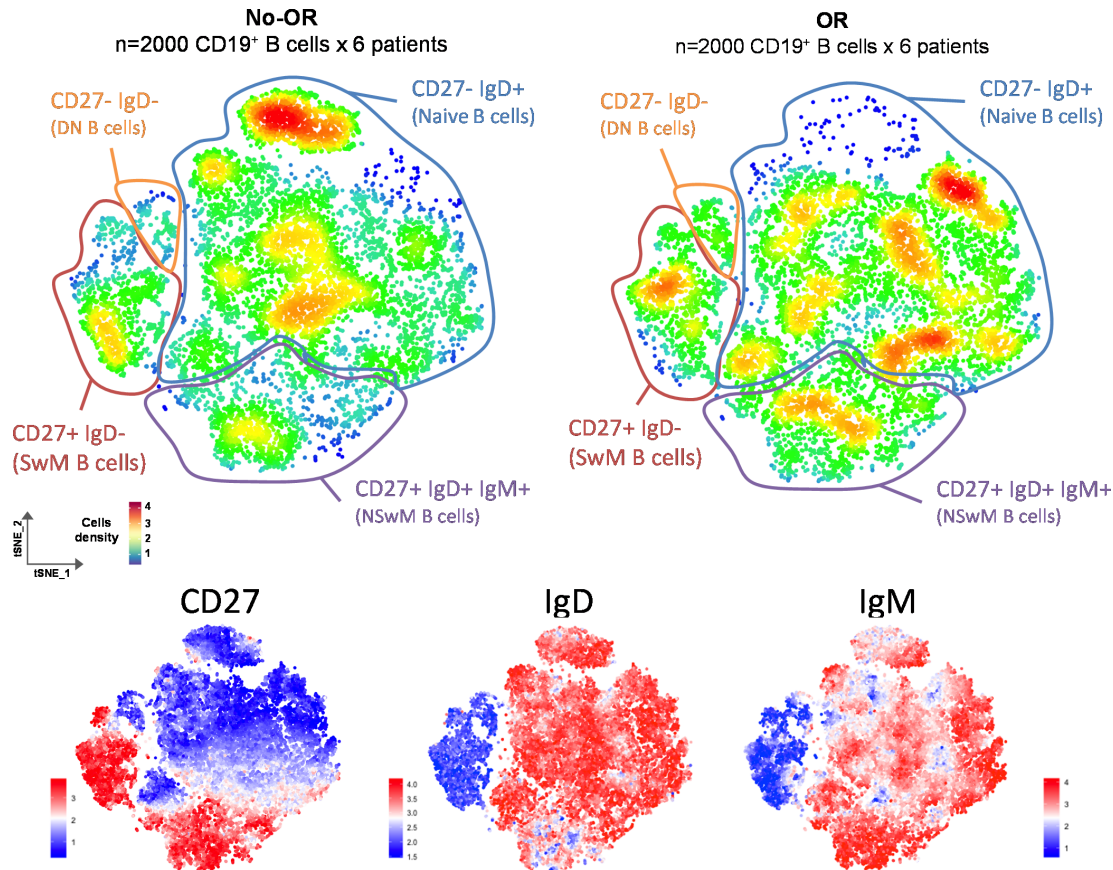


**Figure 1** Density t-SNE plots of baseline B cells subpopulations according to response to nivolumab in the discovery cohort. DN B cells, double negative B cells; NSwM B cell, unswitched memory B cells; SwM B cells, switched memory B cells; t-SNE, t-distributed stochastic neighbor embedding.

Therefore, the assessment of CD27, IgD and IgM expression on circulating B cells by supervised analysis of flow cytometry data were subsequently extended to a larger set of patients (discovery cohort,  $n=44$ ) to confirm these preliminary findings (online supplemental figure S2 for the gating strategy). As shown in figure 2, baseline normalized concentrations of blood NSwM, SwM and DN B cells were significantly higher in responders compared with non-responders ( $p=0.006$ ,  $p=0.046$  and  $p=0.032$ , respectively). In contrast, no statistical differences were observed for normalized concentrations of total B cell counts or naïve B cells between both groups at baseline ( $p=0.182$  and  $p=0.083$ , respectively) (figure 2B). Additionally, we monitored B cell concentrations change from baseline to 1 month of therapy (C3) and to the EOT (C7). No significant changes in concentration levels of all B cell subsets were observed during treatment (figure 2C).

#### Circulating NSwM B cells are associated with clinical outcomes to nivolumab in m-ccRCC

As B cell subpopulations at baseline were associated with response, we next determined if baseline concentrations of these populations could predict survival outcomes to nivolumab in the discovery cohort. Median follow-up was 30 months (95% CI: 17.0 to 21.0)

and median OS was not reached. Considering the median as cut-off value, high NSwM B cell concentration was associated with overall OS, with 1 event out of 22 patients at the time of data cut-off, versus 10 events out of 21 patients with NSwM B cell concentration below the median (12 months OS rate:  $\geq$ median 100% vs  $<$ median: 66.3% (95% CI: 42.0 to 82.3);  $p=0.002$ ) (figure 3A). Moreover, PFS was longer in patients with NSwM B cells over the median (median PFS: 6.8 months; 95% CI: 4.0 to 10.16) compared with those below the median (median PFS: 1.8 months, 95% CI: 1.8 to 4.6;  $p=0.048$ ) (figure 3B). Naïve B cell concentration was associated with OS ( $p=0.043$ ) (figure 3C) but not PFS ( $p=0.237$ ) or response ( $p=0.1$ ). No association with OS or PFS was observed for other B cell subsets (online supplemental figure S3).

#### Correlation between circulating NSwM B cells and tumor-associated TLS

Based on our results and on recently reported studies supporting a role of the TLS and B cells within the TLS in the response to ICB, we next evaluated if there was a correlation between circulating NSwM B cells and tumor-associated TLS in the 17 patients of the discovery cohort for whom TIME characterization was available.<sup>17 22 23</sup> By performing correlation analysis, we observed a positive correlation between the

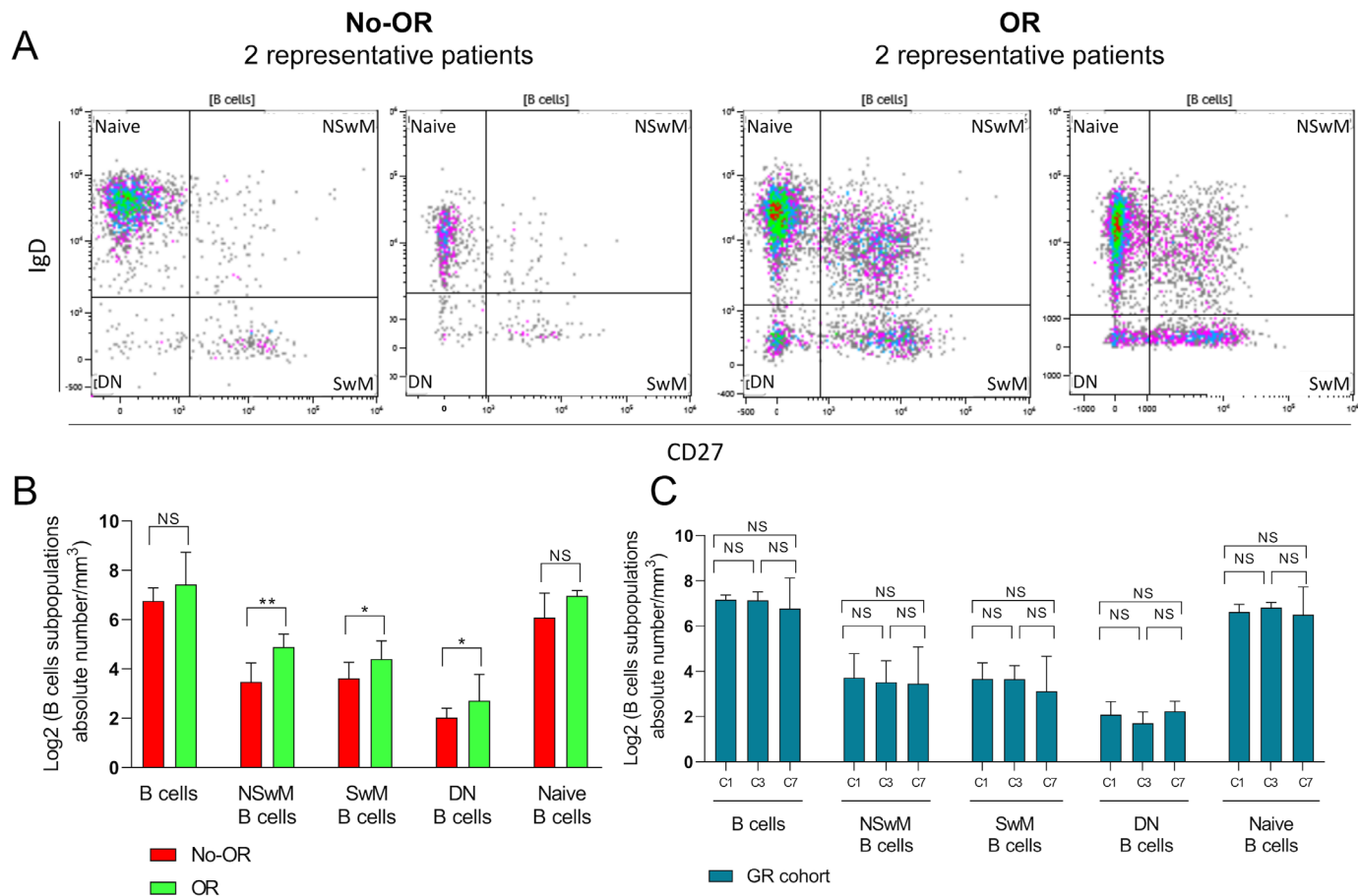


**Figure 2** (A) Representative flow cytometry plots showing the different circulating B cell subsets (naive B cells (CD19+, CD27–, IgD+), double negative B cells (DN B cells, CD19+, CD27–, IgD–) and memory B cells including unswitched (NSwM, CD19+, CD27+, IgD+), switched memory B cells (SwM B cells, CD19+, CD27+, IgD–)) in two No-OR patients and in two OR patients of the discovery cohort. (B) Normalized concentrations of B cells and B cell subpopulations between No-OR and OR patients of the discovery cohort. (C) As in (B) but histograms showing normalized concentrations at baseline (C1), 1 month post-treatment initiation (C3) and at end of nivolumab treatment (C7). DN B cells, double negative B cells; NSwM B cells, unswitched memory B cells; SwM B cells, switched memory B cells.

concentration of circulating NSwM B cells and the number of TLS and CD20+ ( $r=0.59$ ,  $p=0.044$ , and  $r=0.52$ ,  $p=0.033$ , respectively) in the tumor center; a non-significant trend for a positive correlation with the density of TLS was also observed ( $r=0.48$ ,  $p=0.119$ ) (figure 4A). NSwM B cells did not correlated with infiltrating CD8 +T cells in the invasive margin (IM) nor the tumor center ( $r=0.23$ ,  $p=0.492$  and  $r=0.23$ ,  $p=0.383$ ) (figure 4A).

### Circulating T follicular helper cells correlate with NSwM B cells and tumor-associated TLS

Memory T follicular helper cells (Tfh) are critical for germinal center formation and provide growth factors to B cells inducing their differentiation into long-lived plasma cells and memory B cells.<sup>32</sup> Tfh cells are also found in peripheral blood where they associate memory-like functions and there is data suggesting that they could behave as a potential surrogate marker for germinal center reaction.<sup>33–35</sup> In addition, studies suggest that anti-PD-1 therapy could increase circulating Tfh cells enhancing B cell capacity.<sup>35</sup> Thus, we investigated relationship between

circulating NSwM B cells and Tfh as well as Tfh subpopulations at baseline. Supervised analysis of the CD4 +T cell polarization panel was performed<sup>31</sup> (online supplemental figure S4 for the gating strategy).

Significant positive correlation between baseline NSwM B cells and circulating Tfh cells ( $r=0.70$ ,  $p<0.001$ ) was observed. In addition, a significantly higher overall concentration of Tfh cells was observed in responder patients compared with non-responders ( $p=0.027$ ) (figure 4B,C). We next investigated if the baseline concentration of Tfh could predict survival outcomes. The median was considered as the cut-off value. The concentration of Tfh cells at baseline did not correlate with OS ( $p=0.096$ ) or PFS ( $p=0.70$ ). However, Tfh2 and Tfh17DP subpopulations significantly correlated with OS ( $p=0.006$  and  $p=0.007$ , respectively), but not with PFS (figure 4D).

### Impact of TLS on clinical outcomes in patients with m-ccRCC treated with nivolumab

Given our prior results that circulating NSwM B cells were associated with improved survival outcomes and that they also correlated with tumor-associated TLS and CD20 +B

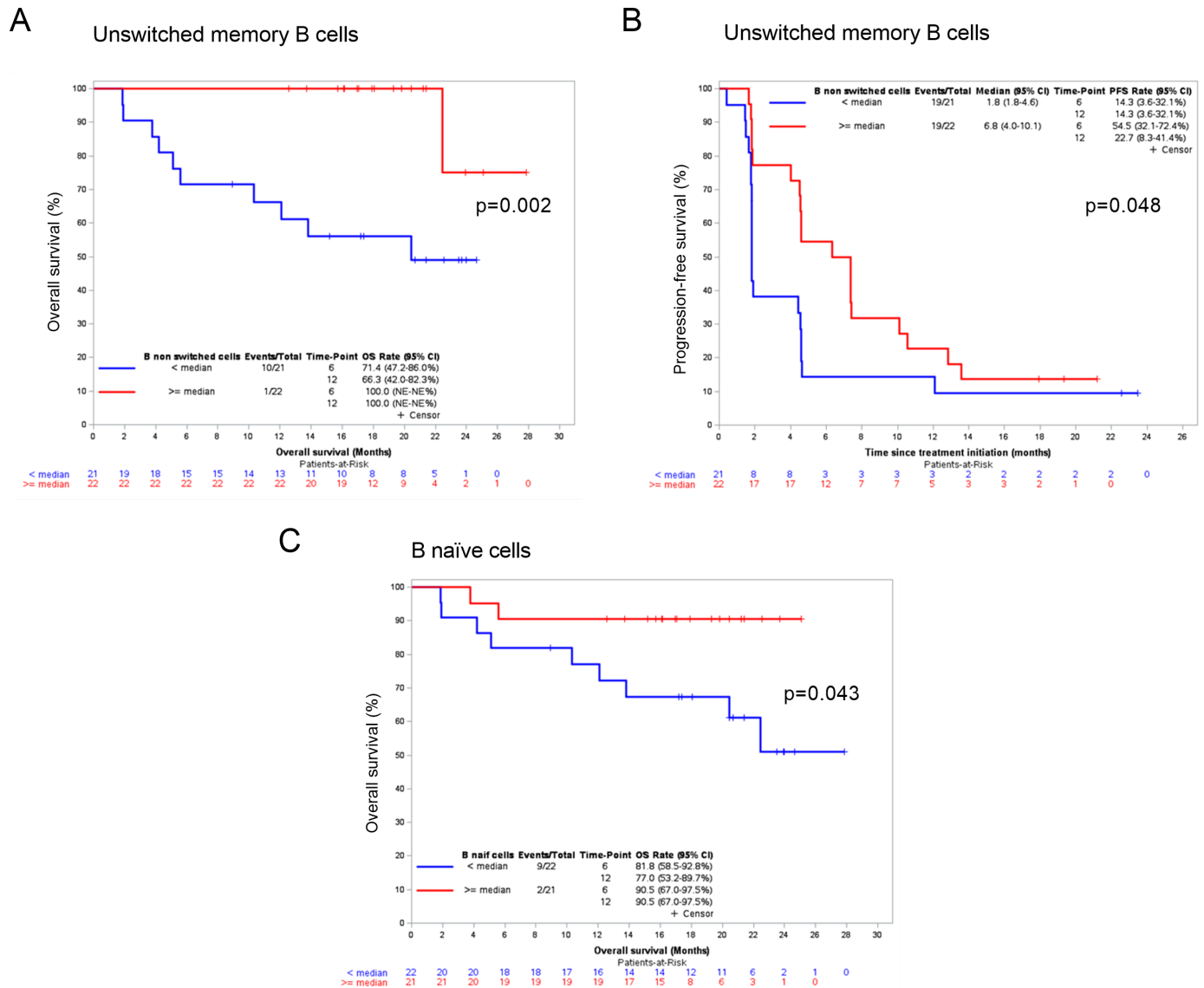


**Figure 3** (A) Kaplan-Meier for OS according to NswM B cells concentration levels (high:  $\geq$ median; low:  $<$ median) in patients with m-ccRCC treated with nivolumab. (B) Kaplan-Meier for PFS according to NswM B cells concentration levels (high:  $\geq$ median; low:  $<$ median) in patients with m-ccRCC treated with nivolumab. (C) Kaplan-Meier for OS according to naïve B cell concentration levels in patients with m-ccRCC treated with nivolumab. m-ccRCC, metastatic clear cell renal cell carcinoma; NswM B cell, unswitched memory B cells; OS, overall survival; PFS, progression-free survival.

cells, we decided to evaluate the association between TLS and clinical outcomes in patients with m-ccRCC treated with nivolumab ( $n=324$ ). Considering a median cut-off value of 2, responses were significantly more frequent in tumors with  $\geq 2$  TLS compared with those with  $< 2$  TLS ( $p=0.043$ ) (figure 5A). The presence of TLS was not predictive of OS ( $p=0.125$ ) nor PFS ( $p=0.074$ ), although a trend for better OS and PFS with higher density of TLS was seen (figure 5B,C).

#### NswM B cells correlate with circulating soluble factors

Soluble factors, including cytokines, chemokines, and soluble proteins, have a crucial role in the immune response and oncogenesis. Variations in the concentration of circulating soluble proteins are the result of production by tumor cells, immune cells and the tumor-immune

cells interactions.<sup>36 37</sup> Thus, given our results supporting the role of NswM B cells in the response to nivolumab in patients with m-ccRCC, we investigated certain soluble factors involved in inflammation as well as T and B cells biology (VEGF, VCAM-1, IL-6, IL-7, IL-8, IL-10, APRIL, BAFF, 4-1BB, BCA-1/CXCL13, SDF-1 $\alpha$ , MDC, IFN- $\gamma$ , and TNF- $\alpha$ ). Interestingly, higher baseline levels of BAFF, implicated in early B cell survival and maturation, and BCA-1/CXCL13, key for the homeostatic orchestration of B cell zones in secondary lymphoid tissue, were significantly inversely correlated with circulating NswM B cells ( $r=-0.42$ ,  $p=0.007$ ; and  $r=-0.55$ ,  $p<0.001$ , respectively) (figure 6A,B). Moreover, BCA-1/CXCL13 did also inversely correlate with circulating Tfh cells at baseline ( $r=-0.61$ ,  $p<0.001$ ) (figure 6B).

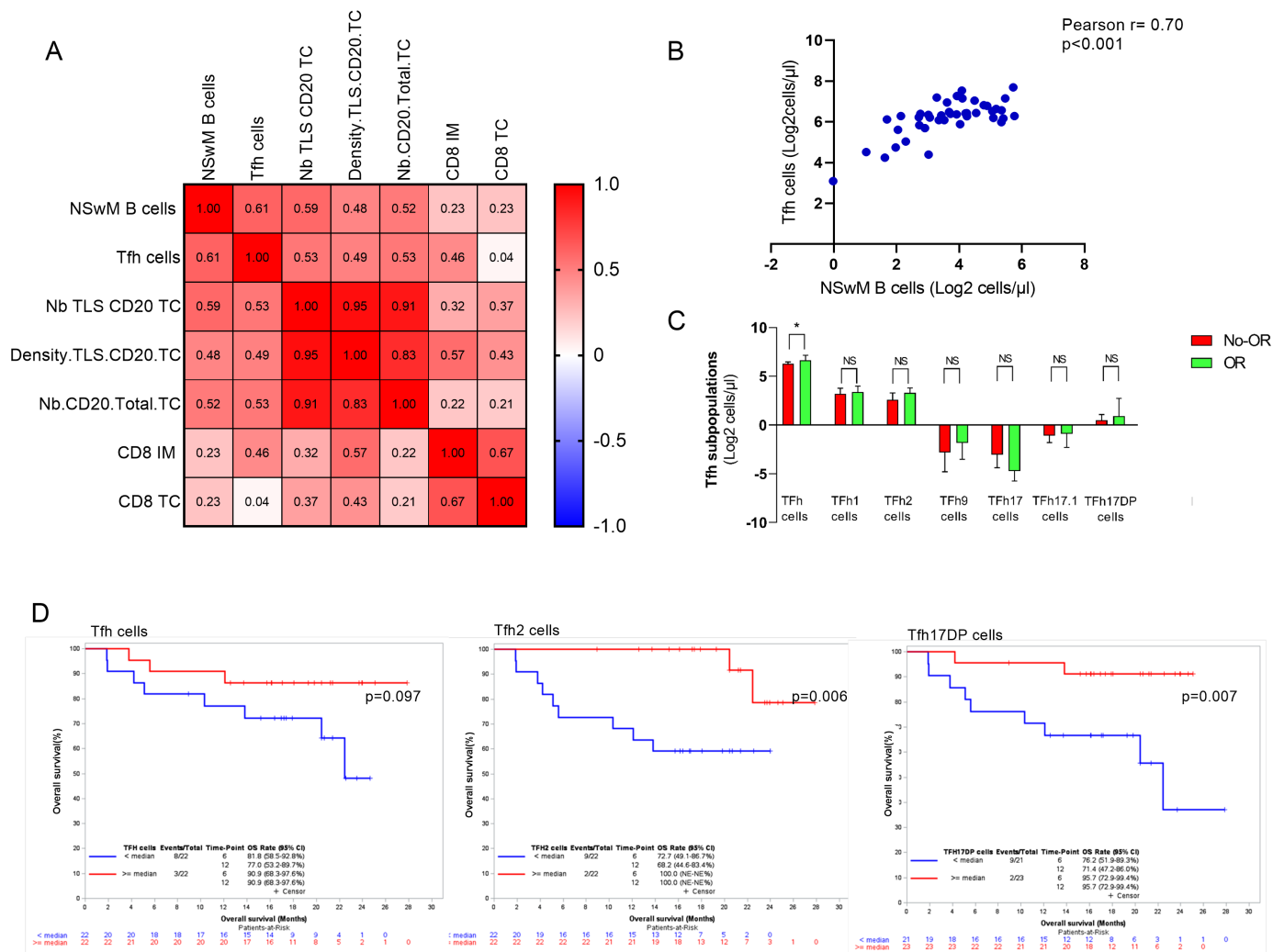


**Figure 4** (A) Correlation heatmap of log<sub>2</sub> transformed count values of circulating NSwM B cells, circulating Tfh cells, tumor-associated TLS (numbers (Nb) and density), CD20 + cell numbers (Nb CD20) and cytotoxic CD8+ (n=17) in tumor center (TC) or invasive margin (IM). (B) Correlation between circulating Tfh cells and NSwM B cells (n=43). Of note only 43 patients out of the 44 analyzed underwent correlation analysis as there was one patient for which we did not have the B cell immunophenotyping (only Tfh). (C) Log<sub>2</sub> transformed count values of Tfh cells and Tfh subsets between responders (OR) and non-responders (No-OR). (D) Kaplan-Meier for overall survival according to blood cells concentration levels of Tfh, Tfh2 and Tfh17DP (high  $\geq$ median, low  $<$ median) (n=44). NSwM B cells, unswitched memory B cells; Tfh, T follicular helper; TLS, tertiary lymphoid structures.

### Correlation between circulating soluble factors and the tumor microenvironment

Given the correlation of circulating NSwM B cells with both TLS and certain circulating soluble factors (BAFF, BCA-1/CXCL13) we then investigated the correlation between the 14 circulating soluble factors and the presence of TLS. A non-significant trend for an inverse correlation between BAFF and the density of TLS ( $r = -0.37$ ,  $p = 0.161$ ) and the number and density of CD20 + cells at the tumor center ( $r = -0.36$ ,  $p = 0.165$ , and  $r = -0.49$ ,  $p = 0.057$ , respectively) was observed. IL-6 also presented a trend for an inverse correlation with the number and density of tumor-associated CD20 + cells ( $r = -0.37$ ,  $p = 0.161$ , and  $r = -0.36$ ,  $p = 0.171$ ). The correlation between circulating soluble factors and tumor infiltrating CD8 + T cells was also evaluated but in very few samples (n=12). Higher levels of IL-6 and IL-10 were significantly positively correlated with

the presence of CD8 + T cells at the IM ( $r = 0.62$ ,  $p = 0.033$ , and  $r = 0.71$ ,  $p = 0.009$ , respectively), while IFN-gamma was negatively correlated ( $r = -0.59$ ,  $p = 0.04$ ).

### B cell-related soluble factors are associated with OS in m-cRCC treated with nivolumab

Cytokine levels have been evaluated as predictors of response to antiangiogenics in mRCC, however data regarding cytokine levels and prediction of response to ICB are still lacking.<sup>38-40</sup> To address this, we next evaluated the association between baseline soluble factors concentration levels and clinical outcomes in the discovery cohort. The soluble factors' quantification analysis was only performed in 40 of the 44 patients included in the discovery cohort. Consistent with our previous results, and considering the 75th percentile (P75) as cut-off value, higher baseline concentration levels of BAFF



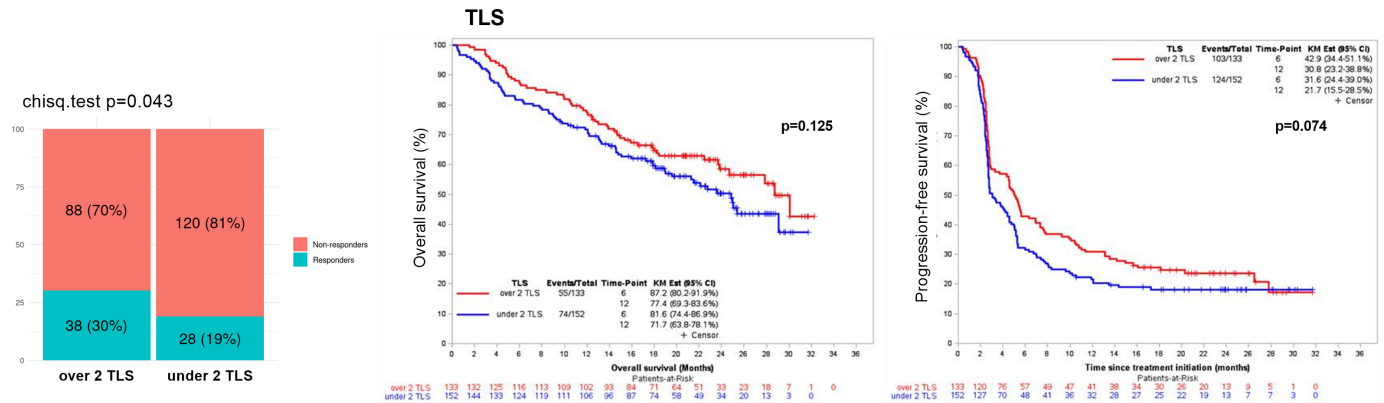


**Figure 5** TLS enrichment was tested with the  $\chi^2$  test between responders and non-responders (left panel). Kaplan-Meier for overall survival (middle panel) and progression-free survival (right panel) according to tumor-associated TLS numbers (over 2 TLS :  $\geq 2$  TLS, under 2 TLS :  $< 2$  TLS) in patients with metastatic clear cell renal cell carcinoma treated with nivolumab. TLS, tertiary lymphoid structures.

and BCA-1/CXCL13, involved in the survival and recruitment of B cells, and of IL-6, involved in inflammation but also in the generation of humoral immunity, were significantly associated with worse OS (HR: 4.39, 95% CI: 1.26 to 15.32,  $p=0.011$ ; HR 4.74, 95% CI: 1.35 to 16.64,  $p=0.008$ ; and HR: 4.41, 95% CI: 1.26 to 15.43,  $p=0.011$ ) (figure 6C); however they did not show a significant statistical association with PFS.<sup>41–45</sup> No other associations with OS or PFS were seen (online supplemental table S3). None of the 14 investigated soluble factors was predictive of response (online supplemental table S4).

Based on these results, BAFF, BCA-1/CXCL13 and IL-6 were then tested in an independent data set including the remaining patients of the NIVOREN translational study with available plasma sample (validation cohort,  $n=313$ ). Using the same cut-off as in the discovery cohort, we confirmed the association of BAFF, BCA-1/CXCL13 and IL-6, with worse OS (BAFF HR: 1.73, 95% CI: 1.21 to 2.46,  $p=0.002$ ; BCA-1/CXCL13 HR: 1.52, 95% CI: 1.08 to 2.15,  $p=0.017$ , and IL-6 HR: 2.53, 95% CI: 1.81 to 3.53,  $p<0.0001$ ). IL-6 did also demonstrate a significant correlation with worse PFS (HR:1.53, 95% CI: 1.16 to 2.03,  $p=0.0024$ ) (figure 6D).

## DISCUSSION

The results of recent studies have brought to light B cells as a major player of the antitumor immune response.<sup>17 22–25</sup> B cells can be found in the tumor and are commonly organized into ectopic lymphoid aggregates with germinal center containing Tfh and CD23 +follicular dendritic cells juxtaposing a T cell zone with mature dendritic cells, known as TLS.<sup>21</sup> Encouraging results of five recent studies support the role of B cells within the TLS in driving antitumor responses in patients with melanoma, sarcoma, m-ccRCC, urothelial, lung and bladder cancer treated with ICB therapy.<sup>17 22–25</sup> However, despite the increasing interest on the B cell compartment, data regarding circulating B cell subpopulations and response are still scarce.<sup>17 30 46</sup> In our study we investigated the

association of circulating B cell subpopulations with response to nivolumab in m-ccRCC. As it has recently been reported in NSCLC,<sup>35</sup> we found that pre-existing high levels of NSwM B cells (CD19 +CD27+IgD+IgM+) were associated with a higher proportion of response, and with improved OS and PFS, in patients with m-ccRCC treated with nivolumab within the GETUG-AFU 26 NIVOREN trial. NSwM B cells significantly correlated with TLS and circulating Tfh cells, which also correlated with TLS, suggesting the relevance of an interplay between B and Tfh cells in the context of PD-1 inhibition that could promote TLS formation and/or maturation. A further analysis demonstrated an inverse correlation between soluble factors involved in B cell survival and recruitment and NSwM B cells (BAFF and BCA-1/CXCL13) and Tfh cells (BCA-1/CXCL13) reinforcing this hypothesis. Further, BAFF, BCA-1/CXCL13 and IL-6, also involved in B cell development and recruitment, were associated with worse OS. NSwM B cells emerge as the first potentially predictive circulating biomarker of response to nivolumab in m-ccRCC.

NSwM B cells consist of a type of memory B cells that have not undergone class switching.<sup>47–49</sup> It seems that on antigen rechallenge NSwM B cells (CD19 +CD27+IgD+IgM+) enter the germinal centre (GC) in contrast to IgG +memory B cells which differentiate to plasma cells.<sup>49</sup> NSwM B cell are low affinity memory B cells that retain an adaptability potential and thus represent a reservoir of rapid-to go polyreactive pool of memory B cells. Circulating NSwM B cells could therefore represent an early line of defense, with the ability to mediate bacteria elimination through IgM neutralization and complement-mediated killing but also enhance the phagocytosis and killing of IgG/IgA opsonized bacterial or tumor cells.<sup>50</sup> Interestingly, NSwM B cells have been reported to be predictive of earlier COVID-19 recovery.<sup>51</sup> Moreover, in this study they observed a strong correlation between NSwM B cells and IgG1/IgM responses to the SARS-CoV-2 spike protein-receptor binding-domain, reinforcing the

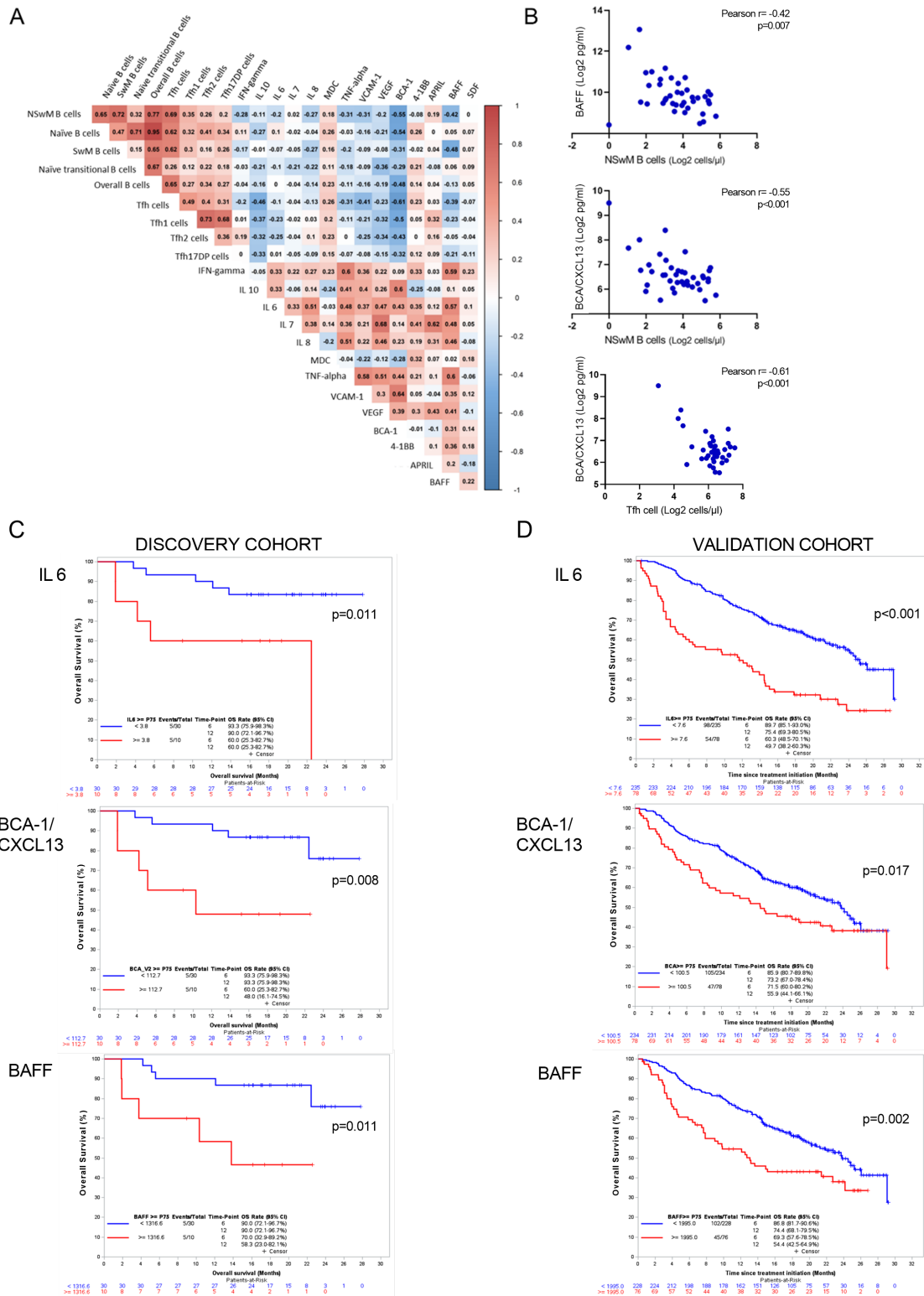


**Figure 6** (A) Correlation heatmap of log2 transformed count values of the B, Tfh subpopulations, and soluble factors. (B) Correlation between blood NSwM B cells and BAFF (upper panel) and BCA-1/CXCL13 (middle panel), and correlation between Tfh cells and BCA-1/CXCL13 (lower panel). (C) Kaplan-Meier for OS according to IL-6 (upper panel), BCA-1/CXCL13 (middle panel) and BAFF (lower panel) concentration levels (high  $\geq P75$ , low  $< P75$ ) in the DISCOVERY cohort (n=40). (D) Kaplan-Meier for OS according to IL-6 (upper panel), BCA-1/CXCL13 (middle panel) and BAFF (lower panel) concentration levels (high  $\geq P75$ , low  $< P75$ ) in the VALIDATION cohort (n=313). Of note, 1 patient out of 313 patients of the VALIDATION cohort was not tested for BCA-1/CXCL13 (n=312), and 9 patients out of 313 were not tested for BAFF (n=304) due to lack of sample. IFN, interferon; IL, interleukin; VEGF, vascular endothelial growth factor; VCAM-1, vascular cell adhesion molecule; MDC, macrophage-derived chemokine; SDF-1, stromal cell-derived factor 1; NSwM B cells, unswitched memory B cells; OS, overall survival; Tfh, T follicular helper; TNF, tumor necrosis factor.

idea of the versatility of this B cell subpopulation.<sup>51</sup> More recently, Xia and colleagues showed for the first time the association between IgM +memory B cells (assimilated to NSwM B cells) and response to anti-PD-1 monotherapy in NSCLC.<sup>30</sup> In line with their results, we found that baseline concentration of circulating NSwM B cells in our study was predictive of response, PFS and OS in patients with m-ccRCC treated with nivolumab (anti-PD-1 therapy). In our study, TLS in the primary tumor, removed sometimes years before in patients, could correlate with NSwM B cells, even though they had received tyrosine kinase inhibitor (TKI) treatment prior to nivolumab. The delay between the primary tumor removal (TLS) and the blood samples is a limitation of our study. However, this peculiar subset of B cells is described as a key memory B cells for 'remembrance of things past'.<sup>47</sup> It is known that contrary to SwM B cells, NSwM B cells which contain few somatic hypermutation, have the ability to produce GC B cells and to persist and become the reservoirs of durable memory.<sup>48</sup> SwM B cells prevail during the early phase of immune memory; however, once SwM B cells disappear due to a short life span, NSwM B cells take on and lead the later phases of memory response.<sup>48</sup> For these reasons, we hypothesized that NSwM B cells may behave as a peripheral imprint of the TLS and tumor microenvironment immune status. However, more robust data are needed to confirm this hypothesis.

Tfh cells are mainly localized in the GC, and thus in secondary lymphoid structures and TLS, where they interact and promote the activation of B cells.<sup>34</sup> Tfh cells can also be found in the peripheral blood.<sup>52</sup> Circulating Tfh cells seem to have a memory-like function able to reactivate on antigen rechallenge and they strongly correlate with potent antibody responses.<sup>52</sup> They have been proposed to be a potential surrogate of GC responses.<sup>34</sup> In our study we observed that circulating Tfh cells correlated significantly with both circulating NSwM B cells and TLS in the tumor. In addition, responder patients were enriched in total circulating Tfh cells. Tfh cells failed to significantly correlate with survival but certain subsets of Tfh cells (Tfh2 and TfhD17P) were associated with improved OS. This observation might be of interest since human blood Tfh1 cells are incapable of helping B cells contrary to Tfh2 and Th17.<sup>53</sup>

The baseline peripheral concentration of the chemokine BCA-1/CXCL13, involved in the recruitment of B and Tfh cells to the GC,<sup>54</sup> was inversely correlated with the concentration of circulating NSwM B cells and Tfh cells, and consequently with worse OS. Our results in the context of recent studies showing that tumor CXCL13 expression correlates with improved survival outcomes to ICB therapy<sup>55 56</sup> suggest that tumor BCA-1/CXCL13 could increase at the expense of a decrease in the levels of circulating BCA-1/CXCL13. This could be enhanced under anti-PD-1 therapy, as Tfh cells highly express PD-1 in lymphoid organs, which seems to inhibit Tfh cell recruitment into the follicle.<sup>57</sup> Moreover, according to the results of Sanchez-Alonso and colleagues, anti-PD-1

therapy seems to induce not only TLS formation but also may induce the differentiation of naïve CD4 +T cells into circulating Tfh cells.<sup>35</sup> Finally, the induction of TLS maturation may increase TLS associated high-endothelial venule which mediate lymphocyte entry and which have been recently reported to predict response to PD-1 plus CTLA-4 combination immunotherapy in patients with melanoma.<sup>58</sup>

Finally, BCA-1/CXCL13 and BAFF, as well as IL-6, also involved in B cell development, were predictive of worse survival outcomes in m-ccRCC treated with nivolumab. Moreover, in the discovery cohort BAFF presented a trend for an inverse correlation with the presence of TLS and tumor-associated B cells, reinforcing the link between the TIME and the peripheral immunity. Interestingly, IL-6 did positively correlate with the presence of tumor-infiltrating CD8 +T cells, which have been reported to be associated with worse survival outcomes in metastatic renal cell carcinoma.<sup>59</sup> The only two studies evaluating the predictive role of different circulating soluble factors in patients with m-ccRCC treated with ICB showed no baseline markers clearly predictive of clinical outcomes.<sup>28 29</sup> Thus, to our knowledge this is also the first study to show a significant association between the concentration of specific circulating soluble factors and survival outcomes in patients with m-ccRCC treated with ICB.

Finally, in our study, in line with previous results, high-TLS tumors presented a higher chance of response.<sup>17</sup> Although no significant differences in OS or PFS according to the density of TLS were observed, a trend for better outcomes in high-TLS tumors was seen. Interestingly, in line with the results of Sanchez-Alonso and colleagues, the translational study of the NABUCCO trial evaluating preoperative ICB combination in locoregionally advanced urothelial cancer, showed that although the presence of TLS at baseline was not predictive of response, neoadjuvant ICB combination was able to induce TLS formation in all patients achieving pathological complete response.<sup>60</sup> These data further support the hypothesis that ICB therapy may induce TLS formation and thus, enhance the antitumor response.

Our study has several limitations. Multiple statistical tests were used, however given the small number of patients, multiple analysis correction was not performed. Most patients were nephrectomized, and thus primary tumor sample used for TLS evaluation was collected several years prior to baseline blood samples used for the immuno-monitoring. In addition, the heterogeneity of treatment lines and previous therapies could have impacted the immune status and treatment outcomes. Although the fresh whole blood immuno-monitoring included a small number of patients from a single institution, the results of the soluble factors quantification analysis were later confirmed in a large independent data set from the same trial, which adds robustness to our data.

## CONCLUSION

Our study shows for the first time that a pre-existing high number of circulating NSwM B cells is associated with higher probability of response to nivolumab and longer PFS and OS in patients with m-ccRCC. We also showed that NSwM B cells positively correlate with baseline circulating Tfh cells and with the presence of tumor-associated TLS in the previously resected primary tumor. In addition, BCA-1/CXCL13 was inversely correlated with both baseline Tfh and NSwM B cells, as well as with worse OS. These findings suggest that, in the context of the previous reported data, that NSwM B cells may not only contribute to the immune response by extending the B cell capacity with an immediate low-affinity IgM response, but also that there might be an interplay between Tfh and NSwM B cells mediated by CXCL13 that could promote the formation and maturation of TLS under ICB therapy. In addition, we reported for the first time an association between circulating soluble factors (IL-6, BCA-1/CXCL13 and BAFF, involved in B cell development and recruitment) and worse OS in patients with m-ccRCC treated with nivolumab.

Altogether, our results reinforce pre-existing data supporting the role of B cell subsets in the response to ICB therapy in patients with m-ccRCC. NSwM B cells may behave as a peripheral imprint of the TME status. Further studies including a non-ICB cohort are needed to confirm these findings and determine if this subpopulation of B cells could be a predictive biomarker of response to ICB.

## Author affiliations

- <sup>1</sup>Department of Cancer Medicine, Institut Gustave-Roussy, Villejuif, France
- <sup>2</sup>Laboratory for Immunomonitoring in Oncology, Institut Gustave-Roussy, Villejuif, France
- <sup>3</sup>Faculté de Pharmacie, Université Paris-Saclay, Chatenay-Malabry, France
- <sup>4</sup>Centre de Recherche des Cordeliers, Inserm UMR S1138, Paris, France
- <sup>5</sup>Department of Biostatistics, Centre Leon Bernard, Lyon, France
- <sup>6</sup>Laboratoire d'immunomonitoring En Oncologie, Institut Gustave-Roussy, Villejuif, France
- <sup>7</sup>Faculté de Médecine, Université Paris-Saclay, Le Kremlin Bicetre, France
- <sup>8</sup>Service d'Oncologie Médicale, Hôpital Européen Georges Pompidou, Paris, France
- <sup>9</sup>Service Anatomie Et cytologie Pathologiques, CHU, Université de Rennes, Université de Rennes 1, Rennes, France
- <sup>10</sup>Department of Immunology, Gustave Roussy Institute, Villejuif, France
- <sup>11</sup>Leuven Cancer Institute, Leuven, Belgium
- <sup>12</sup>Translational Research, UNICANCER, Paris, France
- <sup>13</sup>GETUG group, Unicancer, Paris, France

**Twitter** Maxime Meylan @maxime.meylan

**Acknowledgements** This work was supported by INSERM, Sorbonne Université, Université de Paris, Ligue Contre le Cancer (Equipe labellisée), CARPEM (Cancer Research for Personalized Medicine) programme of the Sites Intégrés de Recherche sur le Cancer (SIRIC), LabeX Immunooncology, Canceropole Ile de France, INCa (Institut du cancer, PRT-K16-GETUG-AFU26 NIVOREN), Unicancer, Association pour la recherche en thérapies innovantes en cancérologie (ARTIC, BioniKK contract (R17169DD), MM fellowship), and Foncer contre le cancer fond de dotation. We thank the CHIC platform of CRC for help in scanning images.

**Contributors** Study concept and design: LC-A, AD, MM, WHF, CS-F, LA and NC-G. Acquisition and analysis: LC-A, AD, MM, MN, LB, CDO, GL, IC-M, WHF, CS-F, LA and NC-G. Interpretation of the data: all authors. Drafting of the manuscript: LC-A and AD. Critical revision of the manuscript for important intellectual content: all authors. Statistical analysis: CD, AD, IC-M and MM. Study supervision: WHF, CS-F, LA and NC-G. LA and NC-G act as the guarantors for the overall content.

**Funding** PRT-K16-181 and Bristol Myers Squibb.

**Competing interests** YV: honoraria for consultancy: BMS, MSD, Ipsen, Pfizer, Roche; research fundings: BMS, Ipsen, Roche. WHF: consultant for Anaveon, Catalym, Novartis, GSK, Adaptimmune, OSE Immunotherapeutics, Elsalys, Parthenon, Oxford Biotherapeutics, Genenta. BE: honoraria for consultancy: Pfizer, BMS, Ipsen, Aveo, Eisai. LA: grants and honoraria from Pfizer, Novartis, BMS, Ipsen, Roche, AstraZeneca, Amgen, Astellas, Exelixis, Corvus Pharmaceuticals, Peloton therapeutics, MSD and Merck, outside the submitted work. NC-G: sponsored research at Gustave Roussy from AstraZeneca, GSK, Roche, Sanofi, Cytune Pharma. Lectures and educational activities Gilead and Servier. All other authors declare no conflicts of interest.

**Patient consent for publication** Not applicable.

**Ethics approval** This study involves human participants and was approved by Unicancer Ethics Committee, reference number CPP 15 11 71. Participants gave informed consent to participate in the study before taking part.

**Provenance and peer review** Not commissioned; externally peer reviewed.

**Data availability statement** Data are available upon reasonable request. All data relevant to the study are included in the article or uploaded as supplementary information.

**Supplemental material** This content has been supplied by the author(s). It has not been vetted by BMJ Publishing Group Limited (BMJ) and may not have been peer-reviewed. Any opinions or recommendations discussed are solely those of the author(s) and are not endorsed by BMJ. BMJ disclaims all liability and responsibility arising from any reliance placed on the content. Where the content includes any translated material, BMJ does not warrant the accuracy and reliability of the translations (including but not limited to local regulations, clinical guidelines, terminology, drug names and drug dosages), and is not responsible for any error and/or omissions arising from translation and adaptation or otherwise.

**Open access** This is an open access article distributed in accordance with the Creative Commons Attribution Non Commercial (CC BY-NC 4.0) license, which permits others to distribute, remix, adapt, build upon this work non-commercially, and license their derivative works on different terms, provided the original work is properly cited, appropriate credit is given, any changes made indicated, and the use is non-commercial. See <http://creativecommons.org/licenses/by-nc/4.0/>.

## ORCID iDs

Lucia Carril-Ajuria <http://orcid.org/0000-0001-8256-4376>  
 Wolf Herve Fridman <http://orcid.org/0000-0002-1332-0973>  
 Catherine Sautes-Fridman <http://orcid.org/0000-0003-1735-8722>

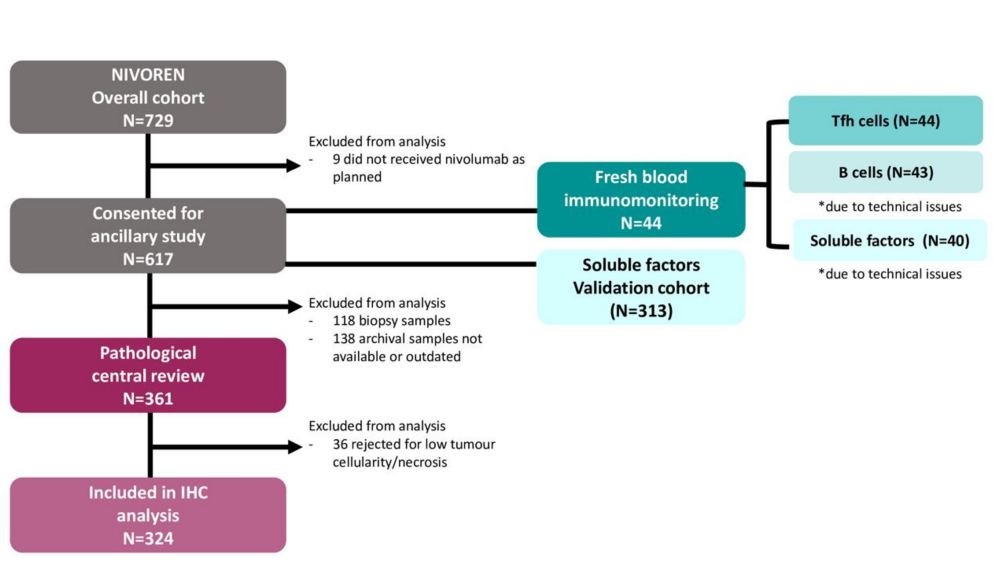
## REFERENCES

- 1 Das S, Johnson DB. Immune-related adverse events and anti-tumor efficacy of immune checkpoint inhibitors. *J Immunother Cancer* 2019;7:306.
- 2 Escudier B, Porta C, Schmidinger M, et al. Renal cell carcinoma: ESMO clinical practice guidelines for diagnosis, treatment and follow-up†. *Ann Oncol* 2019;30:706–20.
- 3 Motzer RJ, Tannir NM, McDermott DF, et al. Nivolumab plus ipilimumab versus sunitinib in advanced renal-cell carcinoma. *N Engl J Med* 2018;378:1277–90.
- 4 Rini BI, Plimack ER, Stus V, et al. Pembrolizumab plus axitinib versus sunitinib for advanced renal-cell carcinoma. *N Engl J Med* 2019;380:1116–27.
- 5 Choueiri TK, Powles T, Burotto M, et al. Nivolumab plus cabozantinib versus sunitinib for advanced renal-cell carcinoma. *N Engl J Med Overseas Ed* 2021;384:829–41.
- 6 Motzer R, Alekseev B, Rha S-Y, et al. Lenvatinib plus pembrolizumab or everolimus for advanced renal cell carcinoma. *N Engl J Med Overseas Ed* 2021;384:1289–300.
- 7 Motzer RJ, Robbins PB, Powles T, et al. Avelumab plus axitinib versus sunitinib in advanced renal cell carcinoma: biomarker analysis of the phase 3 javelin renal 101 trial. *Nat Med* 2020;26:1733–41.
- 8 Braun DA, Hou Y, Bakouny Z, et al. Interplay of somatic alterations and immune infiltration modulates response to PD-1 blockade in advanced clear cell renal cell carcinoma. *Nat Med* 2020;26:909–18.
- 9 Motzer RJ, Banchereau R, Hamidi H, et al. Molecular subsets in renal cancer determine outcome to checkpoint and angiogenesis blockade. *Cancer Cell* 2020;38:S1535610820305420
- 10 Albiges L, Flippot R, Escudier B. Immune checkpoint inhibitors in metastatic clear-cell renal cell carcinoma: is PD-L1 expression useful? *Eur Urol* 2021;79:793–5.

- 11 Strickler JH, Hanks BA, Khasraw M. Tumor mutational burden as a predictor of immunotherapy response: is more always better? *Clin Cancer Res* 2021;27:1236–41.
- 12 McDermott DF, Huseni MA, Atkins MB, et al. Clinical activity and molecular correlates of response to atezolizumab alone or in combination with bevacizumab versus sunitinib in renal cell carcinoma. *Nat Med* 2018;24:749–57.
- 13 Largeot A, Pagano G, Gonder S, et al. The B-side of cancer immunity: the underrated tune. *Cells* 2019;8:449 doi:10.3390/cells8050449
- 14 Meyer C, Cagnon L, Costa-Nunes CM, et al. Frequencies of circulating MDSC correlate with clinical outcome of melanoma patients treated with ipilimumab. *Cancer Immunol Immunother* 2014;63:247–57.
- 15 Chevrier S, Levine JH, Zanotelli VRT, et al. An immune atlas of clear cell renal cell carcinoma. *Cell* 2017;169:736–49.
- 16 Griss J, Bauer W, Wagner C, et al. B cells sustain inflammation and predict response to immune checkpoint blockade in human melanoma. *Nat Commun* 2019;10:4186.
- 17 Helmink BA, Reddy SM, Gao J, et al. B cells and tertiary lymphoid structures promote immunotherapy response. *Nature* 2020;577:549–55.
- 18 Ishigami E, Sakakibara M, Sakakibara J, et al. Coexistence of regulatory B cells and regulatory T cells in tumor-infiltrating lymphocyte aggregates is a prognostic factor in patients with breast cancer. *Breast Cancer* 2019;26:180–9.
- 19 Koh J, Hur JY, Lee KY, et al. Regulatory (FoxP3<sup>+</sup>) T cells and TGF- $\beta$  predict the response to anti-PD-1 immunotherapy in patients with non-small cell lung cancer. *Sci Rep* 2020;10:18994.
- 20 Somasundaram R, Zhang G, Fukunaga-Kalabis M, et al. Tumor-associated B-cells induce tumor heterogeneity and therapy resistance. *Nat Commun* 2017;8:607.
- 21 Sautès-Fridman C, Verneau J, Sun C-M, et al. Tertiary lymphoid structures and B cells: clinical impact and therapeutic modulation in cancer. *Semin Immunol* 2020;48:101406.
- 22 Cabrita R, Lauss M, Sanna A, et al. Tertiary lymphoid structures improve immunotherapy and survival in melanoma. *Nature* 2020;577:561–5.
- 23 Petitprez F, de Reyniès A, Keung EZ, et al. B cells are associated with survival and immunotherapy response in sarcoma. *Nature* 2020;577:556–60.
- 24 Vanhersecke L, Brunet M, Guégan J-P, et al. Mature tertiary lymphoid structures predict immune checkpoint inhibitor efficacy in solid tumors independently of PD-L1 expression. *Nat Cancer* 2021;2:794–802.
- 25 Gao J, Navai N, Alhalabi O, et al. Neoadjuvant PD-L1 plus CTLA-4 blockade in patients with cisplatin-ineligible operable high-risk urothelial carcinoma. *Nat Med* 2020;26:1845–51.
- 26 Yuan S, Liu Y, Till B, et al. Pretreatment peripheral B cells are associated with tumor response to Anti-PD-1-Based immunotherapy. *Front Immunol* 2020;11:563653.
- 27 Ferrara R, Naigeon M, Auclin E, et al. Circulating T-cell immunosenescence in patients with advanced non-small cell lung cancer treated with single-agent PD-1/PD-L1 inhibitors or platinum-based chemotherapy. *Clin Cancer Res* 2021;27:492–503.
- 28 Chehrizi-Raffle A, Meza L, Alcantara M, et al. Circulating cytokines associated with clinical response to systemic therapy in metastatic renal cell carcinoma. *J Immunother Cancer* 2021;9:e002009.
- 29 Martini J-F, Plimack ER, Choueiri TK, et al. Angiogenic and immune-related biomarkers and outcomes following Axitinib/Pembrolizumab treatment in patients with advanced renal cell carcinoma. *Clin Cancer Res* 2020;26:5598–608.
- 30 Xia L, Guo L, Kang J, et al. Predictable roles of peripheral IgM memory B cells for the responses to anti-PD-1 monotherapy against advanced non-small cell lung cancer. *Front Immunol* 2021;12:759217.
- 31 Pitoiset F, Cassard L, El Soufi K. Deep phenotyping of immune cell populations by optimized and standardized flow cytometry analyses: deep immunophenotyping for clinical studies. *Cytometry* 2018;93:793–802.
- 32 Kurosaki T, Kometani K, Ise W. Memory B cells. *Nat Rev Immunol* 2015;15:149–59.
- 33 Hollern DP, Xu N, Thennavan A, et al. B cells and T follicular helper cells mediate response to checkpoint inhibitors in high mutation burden mouse models of breast cancer. *Cell* 2019;179:1191–206.
- 34 Thornhill JP, Fidler S, Klenerman P, et al. The role of CD4<sup>+</sup> T follicular helper cells in HIV infection: from the germinal center to the periphery. *Front Immunol* 2017;8:46.
- 35 Sánchez-Alonso S, Setti-Jerez G, Arroyo M, et al. A new role for circulating T follicular helper cells in humoral response to anti-PD-1 therapy. *J Immunother Cancer* 2020;8:e001187.
- 36 Bridge JA, Lee JC, Daud A, et al. Cytokines, chemokines, and other biomarkers of response for checkpoint inhibitor therapy in skin cancer. *Front Med* 2018;5:351.
- 37 Dranoff G. Cytokines in cancer pathogenesis and cancer therapy. *Nat Rev Cancer* 2004;4:11–22.
- 38 Zizzari IG, Napoletano C, Di Filippo A, et al. Exploratory pilot study of circulating biomarkers in metastatic renal cell carcinoma. *Cancers* 2020;12:92620. doi:10.3390/cancers12092620
- 39 Tran HT, Liu Y, Zurita AJ, et al. Prognostic or predictive plasma cytokines and angiogenic factors for patients treated with pazopanib for metastatic renal-cell cancer: a retrospective analysis of phase 2 and phase 3 trials. *Lancet Oncol* 2012;13:827–37.
- 40 Bilen MA, Zurita AJ, Ilias-Khan NA, et al. Hypertension and circulating cytokines and angiogenic factors in patients with advanced non-clear cell renal cell carcinoma treated with sunitinib: results from a phase II trial. *Oncologist* 2015;20:1140–8.
- 41 Smulski CR, Eibel H. BAFF and BAFF-Receptor in B cell selection and survival. *Front Immunol* 2018;9:2285.
- 42 Arkatkar T, Du SW, Jacobs HM, et al. B cell-derived IL-6 initiates spontaneous germinal center formation during systemic autoimmunity. *J Exp Med* 2017;214:3207–17.
- 43 Rubio AJ, Porter T, Zhong X. Duality of B cell-CXCL13 axis in tumor immunology. *Front Immunol* 2020;11:521110.
- 44 Legler DF, Loetscher M, Roos RS, et al. B cell-attracting chemokine 1, a human CXC chemokine expressed in lymphoid tissues, selectively attracts B lymphocytes via BLR1/CXCR5. *J Exp Med* 1998;187:655–60.
- 45 Muraguchi A, Hirano T, Tang B, et al. The essential role of B cell stimulatory factor 2 (BSF-2/IL-6) for the terminal differentiation of B cells. *J Exp Med* 1988;167:332–44.
- 46 de Jonge K, Tillé L, Lourenco J, et al. Inflammatory B cells correlate with failure to checkpoint blockade in melanoma patients. *Oncimmunology* 2021;10:1873585.
- 47 Palm A-KE, Henry C. Remembrance of things past: long-term B cell memory after infection and vaccination. *Front Immunol* 2019;10:1787.
- 48 Pape KA, Taylor JJ, Maul RW, et al. Different B cell populations mediate early and late memory during an endogenous immune response. *Science* 2011;331:1203–7.
- 49 Akkaya M, Kwak K, Pierce SK. B cell memory: building two walls of protection against pathogens. *Nat Rev Immunol* 2020;20:229–38.
- 50 Cerutti A, Cols M, Puga I. Marginal zone B cells: virtues of innate-like antibody-producing lymphocytes. *Nat Rev Immunol* 2013;13:118–32.
- 51 Newell KL, Clemmer DC, Cox JB, et al. Switched and unswitched memory B cells detected during SARS-CoV-2 convalescence correlate with limited symptom duration. *PLoS One* 2021;16:e0244855.
- 52 He J, Tsai LM, Leong YA, et al. Circulating precursor CCR7(lo) PD-1(hi) CXCR5<sup>+</sup> CD4<sup>+</sup> T cells indicate Tfh cell activity and promote antibody responses upon antigen reexposure. *Immunity* 2013;39:770–81.
- 53 Morita R, Schmitt N, Bentebibel S-E, et al. Human blood CXCR5(+) CD4(+) T cells are counterparts of T follicular cells and contain specific subsets that differentially support antibody secretion. *Immunity* 2011;34:108–21.
- 54 Havenar-Daughton C, Lindqvist M, Heit A, et al. CXCL13 is a plasma biomarker of germinal center activity. *Proc Natl Acad Sci U S A* 2016;113:2702–7.
- 55 Litchfield K, Reading JL, Puttick C, et al. Meta-analysis of tumor- and T cell-intrinsic mechanisms of sensitization to checkpoint inhibition. *Cell* 2021;184:596–614.
- 56 Groeneveld CS, Fontugne J, Cabel L, et al. Tertiary lymphoid structures marker CXCL13 is associated with better survival for patients with advanced-stage bladder cancer treated with immunotherapy. *Eur J Cancer* 2021;148:181–9.
- 57 Shi J, Hou S, Fang Q, et al. PD-1 controls follicular T helper cell positioning and function. *Immunity* 2018;49:264–74.
- 58 Asrir A, Tardiveau C, Coudert J, et al. Tumor-associated high endothelial venules mediate lymphocyte entry into tumors and predict response to PD-1 plus CTLA-4 combination immunotherapy. *Cancer Cell* 2022;40:S1535610822000046
- 59 Giraldo NA, Becht E, Vano Y, et al. Tumor-infiltrating and peripheral blood T-cell immunophenotypes predict early relapse in localized clear cell renal cell carcinoma. *Clin Cancer Res* 2017;23:4416–28.
- 60 van Dijk N, Gil-Jimenez A, Silina K, et al. Preoperative ipilimumab plus nivolumab in locoregionally advanced urothelial cancer: the NABUCCO trial. *Nat Med* 2020;26:1839–44.

## SUPPLEMENTARY MATERIALS:

### Supplementary Methods:



Supplementary Figure S1. NIVOREN translational study flowchart.

### Sample processing

Blood samples were collected in heparinized tubes for fresh whole blood immune phenotyping and plasma banking. For plasma banking, samples were centrifuged at 800 *g* for 10 minutes and stored at  $-80^{\circ}\text{C}$  until analysis. After thawing, a second centrifugation was performed at 10 000  $\times$  *g* for 10 minutes at  $2-8^{\circ}\text{C}$  to remove platelets before conducting cytokine, soluble factors, and growth factors dosage.

## **Fresh whole blood immunophenotyping**

Immune phenotyping was realized at the Laboratory of Immunomonitoring in Oncology (L.I.O.) of the Gustave Roussy Cancer Campus.

To avoid the loss or reduction or phenotype modifications due to the process of freezing/thawing and to reduce technical manipulations and the blood sampling needed to perform the tests, we performed fresh whole blood immune cell phenotyping. To ensure feasibility and reproducibility for use in longitudinal clinical studies, we designed and optimized the marker and dye selections of 6 10-colors flow cytometry panels to use in clinical research studies as previously described (39): Numeration, B cells, Polarization, Activation, Treg Phenotype and MDSC panels, described in the supplementary table S1.

For surface staining on blood, fresh whole blood (100 µl) was incubated for 20 min at room temperature in the dark with liquid antibodies or in Duraclone® tubes. Erythrocytes lysis was performed adding 1 ml of Versalyse™ (Beckman) containing 25 µl of Fixative Solution (Beckman) for liquid antibodies and 2 ml of Versalyse containing 50 µl of Fixative Solution for Duraclone® tubes. After vortex, tubes were incubated for 20 min at room temperature in the dark. After adding 2 ml of phosphate-buffered saline (PBS) 1X, tubes were centrifuged 5 min at 500g, cells were resuspended in 3 ml of 1X PBS and centrifuged again. The pellet was resuspended in 250 µl of 1X PBS and tubes were analyzed on a Gallios™ flow cytometer (Beckman, 10 colors, 3 lasers).

**Supplementary Table S1.** Flow cytometry panels.



Target – Fluorochrome	Provider	Clone	Reference	Dilution	Panel
<b>CD16 – FITC</b>	Beckman Coulter	3G8	B49215	1/10	Numeration
<b>CD56 – PE</b>	Beckman Coulter	N901	A07788	1:10	Numeration Activation
<b>CD19 – ECD</b>	Beckman Coulter	J3-119	A07770	1/20	Numeration
<b>CD244 – PC5,5</b>	Beckman Coulter	C1.7	B21171	1/40	Numeration MDSC
<b>CD14 – PC7</b>	Beckman Coulter	RMO52	A22331	1/50	Numeration
<b>CD8 APC</b>	Beckman Coulter	B9.11	IM2469	1/50	Numeration
<b>CD4 AA700</b>	Beckman Coulter	13B8.2	B10824	1/50	Numeration
<b>CD3 AA750</b>	Beckman Coulter	UCHT1	A94680	1/100	Numeration
<b>CD15 PB</b>	Beckman Coulter	ASR	A74775	1/10	Numeration MDSC
<b>CD45 KrO</b>	Beckman Coulter	J33	B36294	1/20	Numeration
<b>CD57 FITC</b>	Beckman Coulter	NC1	IM0466U	1/10	Activation
<b>CD160 – PE</b>	Beckman Coulter	BY55	IM3657	1/10	Activation

<b>CD69 ECD</b>	Beckman Coulter	TP1.55.3	6607110	1/10	Activation
<b>CD279 PC5,5</b>	Beckman Coulter	PD1 .3	B36123	1/10	Activation
<b>CD137 PC7</b>	Biolegend	4B4-1	309818	1/20	Activation
<b>CD134 (OX40) – PC5,5</b>	Biolegend	ACT35	350010	1:20	Activation
<b>CD3 – AA700</b>	Beckman Coulter	UCHT1	B10823	1:20	Activation Polarization
<b>CD5 – AA750</b>	Beckman Coulter	BL1a	A78836	1/20	Activation
<b>CD4 – PB</b>	Beckman Coulter	13B8.2	A82789	1/50	Activation Polarization
<b>CD8 – KrO</b>	Beckman Coulter	B9.11	B00067	1/50	Activation
<b>IgD – FITC</b>	Beckman Coulter	IA6-2	B30652	1/50	B cells
<b>CD10 – PE</b>	Beckman Coulter	ALB1	A07760	1/10	B cells
<b>CD5 – ECD</b>	Beckman Coulter	BL1a	A33096	1/20	B cells
<b>CD27 – PC5,5</b>	Beckman Coulter	1A4CD27	B21444	1/20	B cells
<b>CD38 – PC7</b>	Beckman Coulter	LS198-4-3	A54189	1/50	B cells
<b>IgM – APC</b>	Beckman Coulter	SA-DA4	B30654	1/50	B cells
<b>CD19 – AA700</b>	Beckman Coulter	J3-119	A07770	1/20	B cells
<b>CD24 – AA750</b>	Beckman Coulter	ALB9	B10738	1/50	B cells

<b>CD21 PB</b>	Beckman Coulter	BL13	B09982	1/50	B cells
<b>CD32 KrO</b>	Beckman Coulter	2E1	B01177	1/20	B cells MDSC
<b>CXCR3 – FITC</b>	Biolegend	G025H7	353703	1:20	Polarization
<b>CCR10 – PE</b>	R&D Systems	6588-5	FAB3478P	1:10	Polarization
<b>CCR7 – Dazzle</b>	Biolegend	G043H7	353236	1/20	Polarization
<b>CCR6 – PE-Cy5,5</b>	Biolegend	G034E3	353405	1:10	Polarization
<b>CCR4 – PC7</b>	Biolegend	L291H4	359409	1:20	Polarization
<b>CXCR5 – APC</b>	Biolegend	J252D4	356907	1:20	Polarization
<b>CD45RA – AA750</b>	Beckman Coulter	2H4LDH11LDB9	A86050	1:20	Polarization
<b>CD161 – BV510</b>	Biolegend	HP-3G10	339922	1:20	Polarization
<b>CD33 – FITC</b>	Biolegend	HIM3-4	303304	1/20	MDSC
<b>HLA-DR – ECD</b>	Beckman Coulter	Immu-357	IM3636	1/20	MDSC
<b>CD64 – PC7</b>	Beckman Coulter	22	B06025	1/20	MDSC
<b>CD11b APC</b>	Beckman Coulter	Bear1	A87782	1/20	MDSC
<b>CD14 AA700</b>	Beckman Coulter	RMO52	A99020	1/20	MDSC
<b>CD16 – AA750</b>	Beckman Coulter	3G8	A66330	1/50	MDSC

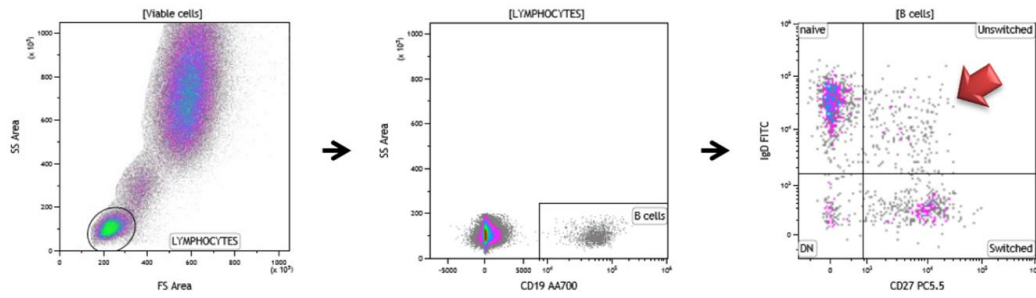
### **Plasma cytokine and soluble proteins concentrations**

Cytokine and soluble proteins concentrations were measured in duplicate in plasma samples using the Meso-Scale Discovery (MSD) immunoassay (Rockville, MD, United States) according to the manufacturer's protocol. Eight different MSD kits were used for each plasma sample: "V-PLEX Human Proinflammatory Panel 1" to measure TNF-alpha, IFN-gamma, IL-6, IL-8 and IL-10, "V-PLEX Human Vascular Injury Panel 2" to measure VCAM-1, "V-PLEX Human Cytokine Panel 1" to measure IL-7 and VEGF, "V-PLEX Human Chemokine Panel 1" to measure MDC, "R-PLEX Human BCA-1/BLC/CXCL13 Assay" to measure BCA-1/CXCL13, "R-PLEX Human APRIL/TNFSF13 Assay" to measure APRIL, "R-PLEX Human 4-1BB/TNFRSF9 Assay" to measure 4-1BB and "U-PLEX Immuno-Oncology Assay" to measure BAFF and SDF-1alpha. Samples were measured using the MESO QuickPlex SQ120 and data, expressed in pg/ml of protein, were analyzed using the DISCOVERY WORKBENCH software (version 4.0). The lower limits of detection (LLOD) are described in Table S2.

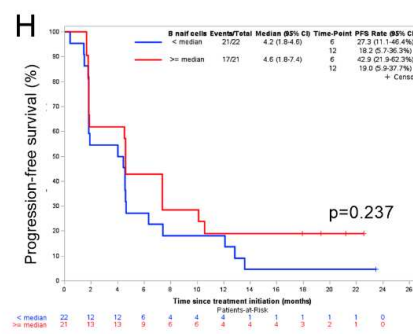
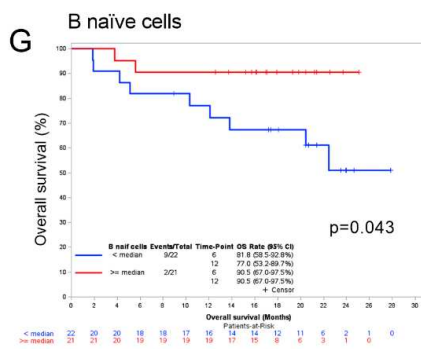
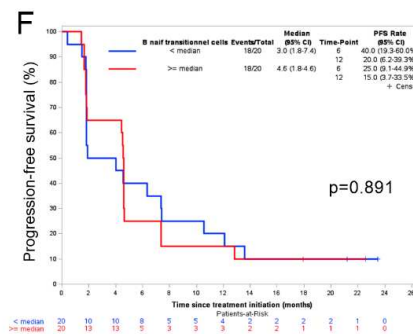
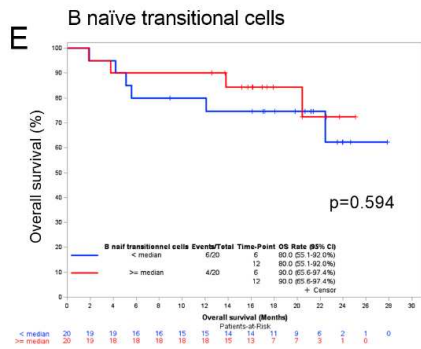
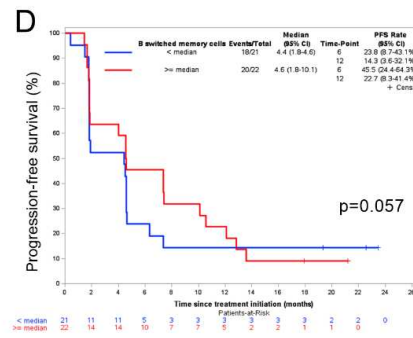
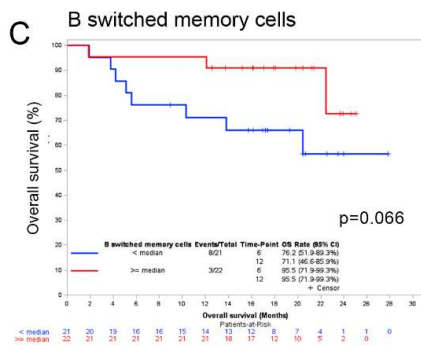
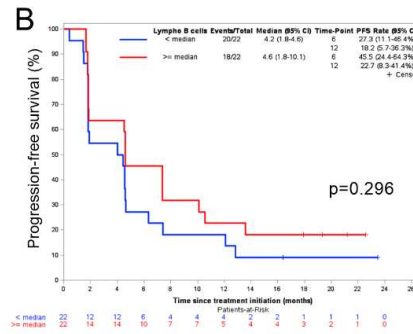
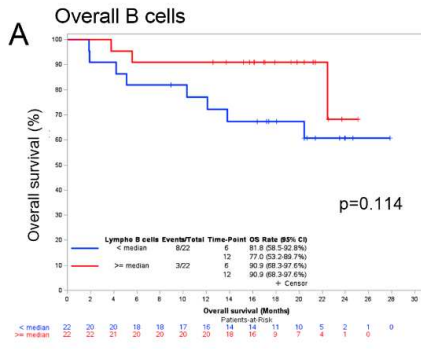
**Supplementary Table S2.** Plasma cytokines and soluble factor's concentration.

Target Cytokine / Soluble protein	Kit	Catalog number	Sample dilution	LLOD	Panel
<b>TNF-alpha</b>	V-PLEX Human Proinflammatory Panel 1	N05049A-1	1:2	0,04 pg/ml	Proinflammatory
<b>IL-6</b>	V-PLEX Human Proinflammatory Panel 1	N05049A-1	1:2	0,06 pg/ml	Proinflammatory
<b>IL-8</b>	V-PLEX Human Proinflammatory Panel 1	N05049A-1	1:2	0,07 pg/ml	Proinflammatory
<b>IL-10</b>	V-PLEX Human Proinflammatory Panel 1	N05049A-1	1:2	0,04 pg/ml	Proinflammatory
<b>IFN-gamma</b>	V-PLEX Human Proinflammatory Panel 1	N05049A-1	1:2	0,37 pg/ml	Proinflammatory
<b>VEGF-A</b>	V-PLEX Human Cytokine Panel 1	N05050A-1	1:2	1,12 pg/ml	Cytokine
<b>IL-7</b>	V-PLEX Human Cytokine Panel 1	N05050A-1	1:2	0,12 pg/ml	Cytokine
<b>VCAM-1</b>	V-PLEX Human Vascular Injury Panel 2	N45198B-1	1:1000	6,00 pg/ml	Vascular Injury

Target Cytokine / Soluble protein	Kit	Catalog number	Sample dilution	LLOD	Panel
<b>MDC</b>	V-PLEX Human Chemokine Panel 1	N05047A-1	1:4	1,22 pg/ml	Chemokine
<b>4-1BB</b>	R-PLEX Human 4-1BB/TNFRSF9	L45SA-1	1:4	1,2pg/ml	4-1BB
<b>APRIL</b>	R-PLEX Human APRIL/TNFSF13	L45SA-1	1:32	87 pg/ml	APRIL
<b>BCA-1/CXCL13</b>	R-PLEX Human BCA-1/BLC	L45SA-1	1:2	1,0 pg/ml	BCA-1/CXCL13
<b>BAFF</b>	U-PLEX Immuno-Oncology	N05227A-1	1:4	0,05 pg/ml	Immuno-Oncology
<b>SDF</b>	U-PLEX Immuno-Oncology	N05227A-1	1:4	278 pg/ml	Immuno-Oncology

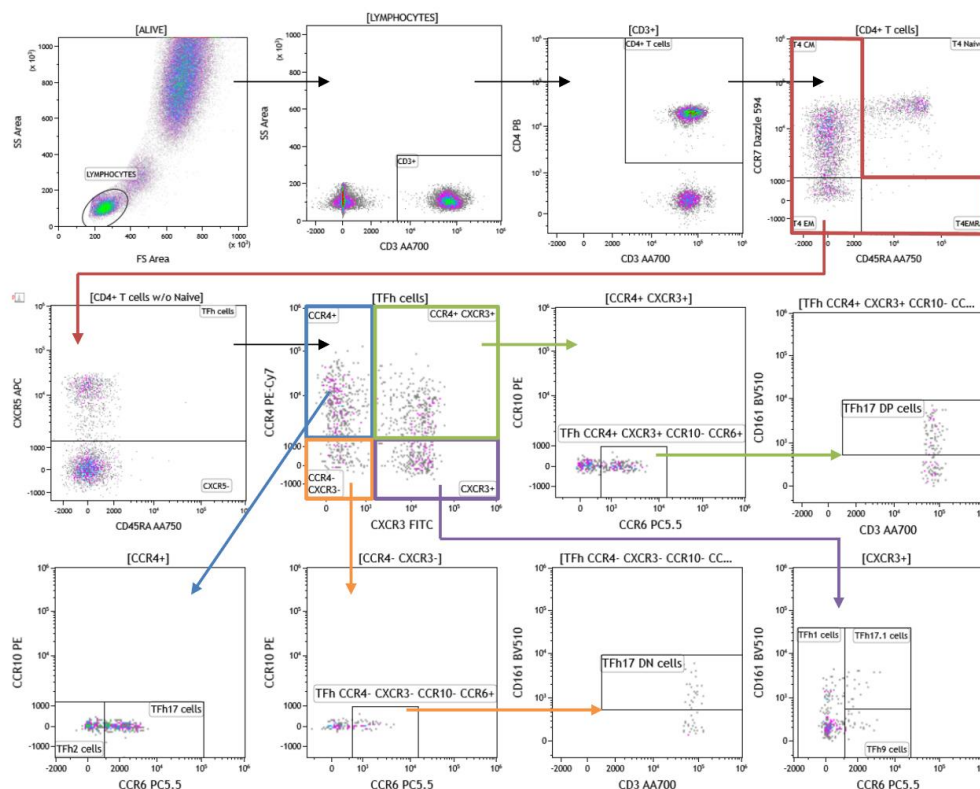
**Supplementary Results:**

**Supplementary Figure S2.** Gating strategy for NSWm B cells (CD19+ CD27+ IgD+ IgM+) according to Pitoiset et al(39).

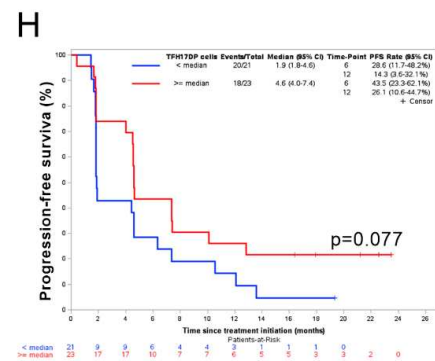
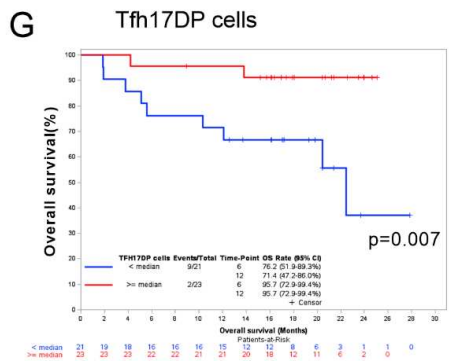
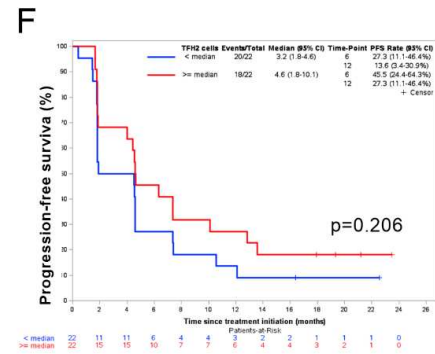
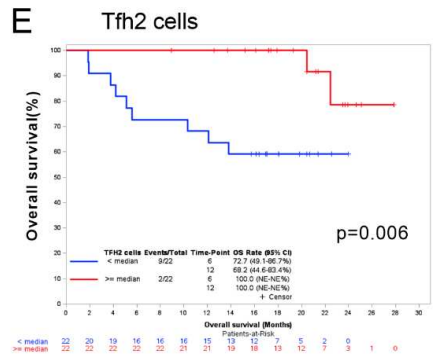
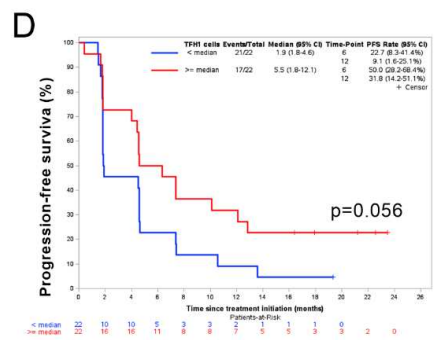
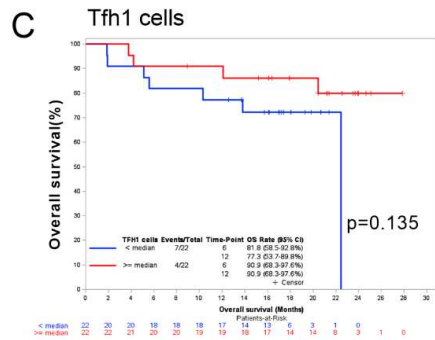
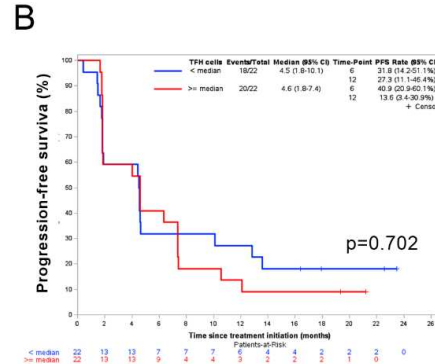
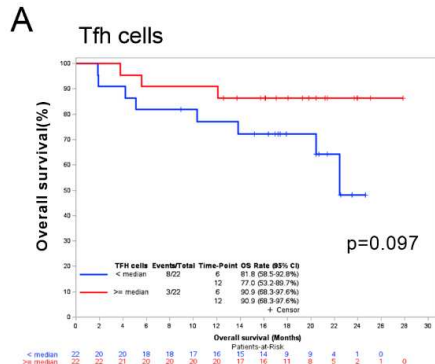




Supplementary Figure S3. (A-B), Kaplan-Meier for OS and PFS according to B cells concentration levels (high:  $\geq$ median; low:  $<$ median) in m-ccRCC patients treated with nivolumab. (C-D), Kaplan-Meier for OS and PFS according to SwM B cells concentration levels (high:  $\geq$ median; low:  $<$ median) in m-ccRCC patients treated with nivolumab. (E-F), Kaplan-Meier for OS and PFS according to naïve transitional B cells concentration levels (high:  $\geq$ median; low:  $<$ median) in mRCC patients treated with nivolumab. (G-H), Kaplan-Meier for OS and PFS according to naïve B cells concentration levels (high:  $\geq$ median; low:  $<$ median) in m-ccRCC patients treated with nivolumab.



Supplementary Figure S4. Gating strategy for Tfh cells.



Supplementary Figure S5. (A-B) Kaplan-Meier for OS and PFS according to TFh cells levels (high:  $\geq$ median; low:  $<$ median) in mRCC patients treated with nivolumab. (C-D) Kaplan-Meier for OS and PFS according to Tfh1 cells levels (high:  $\geq$ median; low:  $<$ median) in mRCC patients treated with nivolumab. (E-F) Kaplan-Meier for OS and PFS according to Tfh2 cells levels (high:  $\geq$ median; low:  $<$ median) in mRCC patients treated with nivolumab. (G-H) Kaplan-Meier for OS and PFS according to Tfh17DP cells levels (high:  $\geq$ median; low:  $<$ median) in mRCC patients treated with nivolumab.

Supplementary Table S3. Discovery cohort. Association between soluble factors concentration levels and OS/PFS.

Cytokines	Selected threshold	OS HR (IC95%)	PFS HR (IC95%)
		p value	p value
<b>IFN</b>	Median	P= 0.9767	P=0.9033
< 6.5	< median	1	1
≥6.5	≥median	0.98 (0.28-3.42)	1.04 (0.53-2.03)
<b>IL10</b>	Median	P=0.0723	P=0.5148
< 0.4	< median	1	1
≥ 0.4	≥ median	3.24 (0.83-12.61)	0.80 (0.41-1.59)
<b>IL6</b>	3 <sup>rd</sup> quartile	<b>P=0.0112</b>	P=0.6459
< 3.8	< Q3	1	1
≥3.8	≥Q3	<b>4.41 (1.26-15.43)</b>	1.19 (0.55-2.55)
<b>IL7</b>	Median	P=0.4302	P=0.1525*
< 5.9	< median		
≥ 5.9	≥ median	1.66 (0.47-5.87)	1.60 (0.81-3.16)
<b>IL8</b>	3 <sup>rd</sup> quartile	P=0.5240	P=0.5493
< 15.9	< Q3	1	1
≥ 15.9	≥ Q3	1.55 (0.40-6.05)	1.26 (0.57-2.80)
<b>MDC</b>	1 <sup>st</sup> quartile	P=0.1283	P=0.3263
< 561	< Q1	1	1
≥ 561	≥ Q3	0.39 (0.11-1.38)	1.50 (0.64-3.50)
<b>MDC</b>	Median	P=0.7810	P=0.1337
< 636.3	< median	1	1
≥ 636.3	≥ median	0.84 (0.24-2.94)	1.64 (0.83-3.21)
<b>TNF</b>	Median	P=0.4646	P=0.1067
< 3.4	< median	1	
≥ 3.4	≥ median	1.61 (0.45-5.81)	0.59 (0.30-1.16)
<b>VCAM 1</b>	3 <sup>rd</sup> quartile	P=0.0714	P=0.8266

< 638470.3	< Q3	1	1
≥ 638470.3	≥ Q3	3.16 (0.84-11.84)	0.92 (0.42-2.03)
<b>VCAM 1</b>	Median	P=0.1973	P=0.2766
< 494344.2	< median	1	1
≥ 494344.2	≥ median	2.39 (0.61-9.39)	0.70 (0.36-1.37)
<b>VEGF</b>	3 <sup>rd</sup> quartile	P=0.6616	P=0.0967
< 63.7	< Q3	1	1
≥ 63.7	≥ Q3	1.36 (0.34-5.36)	1.83 (0.86-3.88)
<b>BCA-1/CXCL13</b>	3 <sup>rd</sup> quartile	<b>P=0.0076</b>	P=0.6285
< 56.3	< Q3	1	1
≥ 56.3	≥ Q3	<b>4.74 (1.35-16.64)</b>	1.21 (0.54-2.68)
<b>4 1BB 2</b>	Median	P=0.4302	P=0.8037
< 58.4	< median	1	1
≥ 58.4	≥ median	1.66 (0.47-5.87)	0.92 (0.47-1.79)
<b>APRIL</b>	Median	P=0.5677	P=0.8280
< 4777.9	< median	1	1
≥ 4777.9	≥ median	0.69 (0.20-2.46)	1.07 (0.55-2.10)
<b>BAFF</b>	3 <sup>rd</sup> quartile	<b>P=0.0114</b>	P=0.9974
< 1316.6	< Q3	1	1
≥ 1316.6	≥ Q3	<b>4.39 (1.26-15.32)</b>	1.00 (0.45-2.21)

Supplementary Table S4. Discovery cohort. Association between soluble factors concentration levels and ORR.

	Objective Response : complete response		Patients	Test
	or partial response			
	No N=32	YES N=7	N=39	
<b>IFN &gt;= P50</b>				Fisher
< 6.5	15 (46.9%)	4 (57.1%)	19 (48.7%)	Exact
≥ 6.5	17 (53.1%)	3 (42.9%)	20 (51.3%)	P = 0.695
<b>IL10 &gt;= P50</b>				Fisher
< 0.4	18 (56.3%)	2 (28.6%)	20 (51.3%)	Exact
≥ 0.4	14 (43.8%)	5 (71.4%)	19 (48.7%)	P = 0.235
<b>IL6 &gt;= P75</b>				Fisher
< 3.8	25 (78.1%)	4 (57.1%)	29 (74.4%)	Exact
≥ 3.8	7 (21.9%)	3 (42.9%)	10 (25.6%)	P = 0.344
<b>IL7 &gt;= P50</b>				Fisher
< 5.9	15 (46.9%)	5 (71.4%)	20 (51.3%)	Exact
≥ 5.9	17 (53.1%)	2 (28.6%)	19 (48.7%)	P = 0.407
<b>IL8 &gt;= P75</b>				Fisher
< 15.9	25 (78.1%)	5 (71.4%)	30 (76.9%)	Exact
≥ 15.9	7 (21.9%)	2 (28.6%)	9 (23.1%)	P = 0.653
<b>MDC &gt;= P25</b>				Fisher
< 561	9 (28.1%)	1 (14.3%)	10 (25.6%)	Exact
≥ 561	23 (71.9%)	6 (85.7%)	29 (74.4%)	P = 0.653
<b>MDC &gt;= P50</b>				Fisher
< 636.3	14 (43.8%)	5 (71.4%)	19 (48.7%)	Exact
≥ 636.3	18 (56.3%)	2 (28.6%)	20 (51.3%)	P = 0.235
<b>TNF &gt;= P50</b>				
< 3.4	18 (56.3%)	2 (28.6%)	20 (51.3%)	

	Objective Response : complete response or partial response		Patients N=39	Test
	No N=32	YES N=7		
	≥ 3.4	14 (43.8%)	5 (71.4%)	19 (48.7%)
<b>VCAM 1 &gt;= P75</b>				Fisher
< 638470.3	26 (81.3%)	3 (42.9%)	29 (74.4%)	Exact P = 0.057
≥ 638470.3	6 (18.8%)	4 (57.1%)	10 (25.6%)	
<b>VCAM 1 &gt;= P50</b>				Fisher
< 494344.2	17 (53.1%)	2 (28.6%)	19 (48.7%)	Exact P = 0.407
≥ 494344.2	15 (46.9%)	5 (71.4%)	20 (51.3%)	
<b>VEGF &gt;= P75</b>				Fisher
< 63.7	23 (71.9%)	6 (85.7%)	29 (74.4%)	Exact P = 0.653
≥ 63.7	9 (28.1%)	1 (14.3%)	10 (25.6%)	
<b>BCA-1/CXCL13 &gt;= P75</b>				Fisher
< 56.3	24 (75.0%)	5 (71.4%)	29 (74.4%)	Exact P = 1.000
≥ 56.3	8 (25.0%)	2 (28.6%)	10 (25.6%)	
<b>4 1BB 2 &gt;= P50</b>				Fisher
< 58.4	17 (53.1%)	3 (42.9%)	20 (51.3%)	Exact P = 0.695
≥ 58.4	15 (46.9%)	4 (57.1%)	19 (48.7%)	
<b>APRIL &gt;= P50</b>				Fisher
< 4777.9	16 (50.0%)	3 (42.9%)	19 (48.7%)	Exact P = 1.000
≥ 4777.9	16 (50.0%)	4 (57.1%)	20 (51.3%)	
<b>BAFF &gt;= P75</b>				Fisher
< 1316.6	23 (71.9%)	6 (85.7%)	29 (74.4%)	Exact P = 0.653
≥ 1316.6	9 (28.1%)	1 (14.3%)	10 (25.6%)	
<b>SDF &gt;302</b>				

	Objective Response : complete response or partial response		Patients N=39	Test
	No N=32	YES N=7		
	< Detection threshold	17 (53.1%)	5 (71.4%)	22 (56.4%)
> Detection threshold	15 (46.9%)	2 (28.6%)	17 (43.6%)	Exact P = 0.438



